Frequency Control via Demand Response in Smart Grid

by

Farid Farmani

A thesis
presented to the University of Waterloo
in fulfillment of the
thesis requirement for the degree of
Master of Applied Science
in
Electrical and Computer Engineering

Waterloo, Ontario, Canada, 2018

Author's Declaration

I hereby declare that I am the sole author of this thesis. This is a true copy of the thesis, including any required final revisions, as accepted by my examiners.

I understand that my thesis may be made electronically available to the public.

Abstract

In order to have a reliable microgrid (MG) system, we need to keep the frequency within an acceptable range. However, due to disturbances in a MG system (such as a sudden load change), it can experience major or minor deviations in frequency, which needs to be reduced within seconds to provide the system stability. In order to maintain the balance between energy supply and demand, traditionally, generation side controllers are utilized to stabilize the power system frequency. These systems add high operational cost, which is not desired for power system operators. With the introduction of smart grid, more and more renewable energy sources are to be used in the power system. The intermittent behavior of these energy resources, as well as high operation cost of conventional controllers, has led to research for new alternatives. In a smart grid environment, demand response (DR) programs can be considered as a promising alternative to the conventional controllers, to efficiently contribute to the frequency regulation by switching responsive loads on or off. DR programs can reduce the amount of energy reserve required and, hence, are more cost efficient. Moreover, they can act very fast and can provide a wide range of operation time from a few seconds to several minutes. Thermostatically controlled loads (TCLs) are proper candidates to participate in frequency regulation programs. However, individual TCLs do not have a noticeable impact on frequency due to small size. They should be aggregated in order to have a considerable effect on frequency. Nevertheless, there are still many challenges which should be addressed in order to make use of TCLs for frequency control in smart grid. In this regard, proper aggregated load models and control algorithms for TCLs contributing to this service need to be investigated.

In this thesis, we present an aggregation model for TCLs and a control strategy to coordinate power provided from DR participants with that of generation side of the MG to keep system frequency within its desired range. For the aggregation model considered in this study, a state space model is used to take into account the interdependency of TCLs' temperature participating in DR programs. The model groups TCLs into clusters, each controlled by an aggregator. A minimum off/on period is considered for individual TCLs to avoid frequent switching of these devices. A control strategy is presented to control frequency by coordinating the generation and demand side regulation service providers. Computer simulation results show that the proposed aggregation model and control strategy can effectively control frequency under various case studies.

Acknowledgements

First and foremost, I would like to express my sincere gratitude to my supervisor, professor Weihua Zhuang for her guidance, patience and support throughout my Master studies. Under her supervision, I have learnt beyond the boundaries of power and energy systems. It has been my honor to have completed my studies under her supervision and she continues to be my role model in professionalism and class throughout my life.

I would also like to acknowledge the readers of my thesis, professor Sherman Shen and professor Oleg Michalovic for their valuable comments to enhance the quality of my work.

I wish to acknowledge professor Shen for his valuable lifetime lessons during the weekly group meetings. I learnt a lot from him and wish to employ his advices throughout my life.

I am always grateful for the support of my friends at BBCR lab. Special thanks to Ahmed, Omar, Hesham, Nan, Jianbing, Mohammed, Joban, and all other BBCR members. Thank you all for creating a pleasant and friendly working environment in the lab.

I would like to thank my best friend, Mehdi, for being an awesome friend, officemate and roommate for the past two years.

Finally, I would like to thank my family for their support and kindness since I was a child until now, my mother Maliheh, my brothers Farshid, Farzad and Vahid and whoever helped me make this possible.

Dedication

This is dedicated to my sweet and loving mother, a strong and gentle soul who taught me to trust in love, believe in hard work and that so much could be done with little.

Table of Contents

List of Tables

List of Figures

List of Acronyms

A/C air conditioner

AHP adaptive hill climbing

BESS battery energy storage system

DADR decentralized active DR

DER distributed energy resource

DG distributed generation

DR demand response

DZ diesel generator

EDR emergency DR

ETP equivalent thermal parameter

EV electric vehicle

EWH electric water heater

FCI frequency control index

HVAC heating ventilation and air conditioning

LC load controller

MC micro-source controllers

MG microgrid

MGCC microgrid central controller

PCC point of common coupling

PV photo-voltaic

RES renewable energy source

TCL thermostatically controlled loads

TCLA thermostatically controlled load aggregator

WT wind turbine

Chapter 1

Introduction

1.1 Microgrid and DR programs

Due to high importance of developing a more efficient, more reliable, and cleaner electric power grid, the traditional energy sector has moved towards the introduction of smart grid. Smart grid commonly refers to the utility electricity delivery system which improves the efficiency, economics, and sustainability of the production and distribution of electricity through the two-way digital communication network and computer processing technology [1]. Within the smart grid, microgrid (MG) is defined as a low-voltage generation/distribution network including a group of distributed energy resource (DER) units such as diesel generator (DZ), solar panels and wind turbine (WT). An MG can operate while connected to the main grid via the point of common coupling (PCC), and also in an islanded mode where it is totally disconnected from the main grid [2, 3]. In the latter mode, keeping the frequency

stability becomes critical as there is no connection to the main grid and the system inertia is lower than that in the grid-connected mode. One of these stability concerns relates to the system frequency. In order to keep the system frequency within a desired range in all conditions, the supply-demand balance must be retained in various situations. However, due to disturbances happening in a power system (e.g., sudden load changes), it can experience major or minor deviations in frequency, which need to be controlled within seconds to provide the power system stability [4]. In order to maintain the balance between supply and demand in a power system, two main levels of control are generally used. Primary frequency control is a local automatic control that adjusts the active power generation and consumption to quickly (within seconds) restore the balance between load and generation [5, 6]. It is noteworthy to mention that this type of control cannot return the frequency to its nominal value, but can arrest the frequency drop and stabilize it. In order to bring the frequency back to its nominal value, secondary control is implemented. The response time of each control type is important to be considered. Secondary control acts within thirty seconds up to a few minutes. The reaction time for primary control is much shorter than that for the secondary control, so the appliances participating in primary control must act very fast. However, the ones participating in secondary control do no need to be fast acting devices [5]. Traditionally, generation side controllers have been utilized to stabilize the power system frequency. These systems add high operational cost, which is not suitable for power system operators. With the introduction of smart grid, more and more renewable energy source (RES)s are used in the power system. The intermittent behavior of these energy resources, as well as high operation cost of

conventional controllers, has made researchers seek for new alternatives. In a smart grid environment, demand response (DR) programs can be considered as a promising alternative to the conventional controllers, to efficiently contribute to the frequency regulation [7, 8]. DR programs can reduce the amount of energy reserve required and, hence, are more cost efficient. Moreover, they can act very fast and can provide a wide range of operation time from a few seconds to several minutes. The frequency control in an MG can be handled by a microgrid central controller (MGCC) which is responsible for ensuring the balance between distributed generation (DG) output power and load consumption in each time horizon from short term of 1 to 24 hours to very short term of 60 seconds or less.

1.2 Motivation and Contribution

As mentioned in subsection 1.1, providing frequency control via DR programs can be a cost efficient alternative for traditional frequency control which is solely performed by generation side. In this regard, there are existing studies to investigate provision of frequency control by the thermostatically controlled loads (TCL)s. Since the power consumption from an individual TCL is not significant, it is imperative to aggregate a large number of these devices in order to have considerable frequency control service. In this regard, the aggregation model embedded in the local aggregator is the foundation for DR programs. A well-desired aggregation model should take into account the low inertia of islanded MG, which means that a fast and comprehensive control strategy needs to be developed. The model should consider coordination of

DR with generation side under various frequency conditions, and intermittent behavior of RES in the system. Moreover, in order to prevent frequent switching of TCLs, minimum off-time and on-time should be considered in the model. Most of the existing works have investigated load following problem in time span of several hours. However, it is important to study frequency regulation in an islanded MG considering all the mentioned issues in scale of seconds. Though there already exist numerous results on controlling TCLs for DR, many problems in aggregation modeling and control remain open. In the islanded MG, load changes and intermittent behavior of RES cause system frequency to deviate from its nominal value. The frequency control system should keep the MG frequency within its acceptable operating range. This should be done by properly incorporating the TCLs in the frequency control, while having coordination with the generation side. Minimizing frequency deviations due to load perturbations/renewable energy intermittency in the MG can be achieved by applying DR with the TCL aggregation model. Due to small impact of an individual TCL on MG control, it is necessary to engage a large number of TCLs into frequency regulation. The problem becomes complex, because not only we deal with a large number of devices, but also we need to ensure the customers' comfort level.

In this thesis, our main objective is to design a TCL aggregation control strategy for MG frequency regulation purposes. Under this aggregation method, heterogeneous TCLs are grouped into several classes. thermostatically controlled load aggregator (TCLA)s are responsible to manage each group of TCLs, and TCLs are prioritized based on their setting temperature statuses. This helps solving the challenge of fre-

quency control via a large number of potential participants, and difficulties in dealing with many small loads rather than a limited number of generating units [4]. When the number of TCLs increases, their heterogeneity increases as well. Hence, aggregating a large number of heterogeneous TCLs becomes challenging and an aggregation model is required to account for their heterogeneity [9–11]. In our study, we apply the aggregation model proposed in [12] as a basis to take advantage of TCLs for fast frequency regulation. In order to make our control strategy fast enough for low inertia islanded MGs, a direct relation between TCL temperature and system frequency is considered to provide fast regulation service.

The contributions of this thesis include prioritizing the TCLAs instead of individual TCLs, which takes into account the thermal dependency of TCLs within aggregation model. Existing aggregation models such as the one in [12] have been mainly proposed for load following purposes and the relative case studies are in a time scale of minutes to several hours. To the best of the our knowledge, this study is one of the very few studies which deal with fast regulation performed by aggregated TCLs in islanded MGs in order of seconds. Moreover, we consider the coordination of generation (renewable-non-renewable) and DR in an islanded MG instead of simply using the load-supply balancing signal from the power system operator. In addition, we consider the lockout effect of individual TCLs to make the model more cost efficient and reliable.

1.3 Outline

The reminder of this thesis is organized as follows. Chapter 2 provides a literature review on control strategies and aggregation TCL models. Chapter 3 presents the system model of our research work. We also present the proposed aggregation model, the temperature-dependent frequency control strategy, and the complete problem formulation. The performance evaluation of the proposed scheme is provided in Chapter 4. We analyze the TCL aggregation control strategy under both over-frequency and under-frequency modes. We also investigate the lock-out effect of TCLs in those cases. Moreover, the system performance under intermittent behavior of the RES is discussed. Finally, Chapter 5 draws the conclusion and identifies the future work of this research.

Chapter 2

Literature Survey

2.1 Introduction

With unceasing renewable energy and power consumption of the consumers within the power system, more stress has been put on the regulating generators to maintain supply-demand balance of the system. In addition, regulating generators are not working at their preferred working point which is not desired for the system operator [13]. On the other had, making the regulating generator change its output frequently in response to frequency deviation signal, puts a lot of pressure on the mechanical equipment leading to shortened lifetime of the generators. As discussed in Chapter 1, DR programs are the most promising alternative for regulating generators to provide regulation services. For this purpose, TCL is a type load that can be controlled via its setting temperature to reduce or increase the power consumption for demand-supply balancing purposes. The capability of aggregate power consumption of TCLs

to provide load balancing service is confirmed in [13, 14]. A battery model showing that flexible loads such as TCLs are good candidates for ancillary services. As discussed in Chapter 1, one of the challenges in implementing regulation service via TCLs, is to define their aggregate dynamics to have significant impact on the power supply-demand balance. In this chapter a literature survey on DR via TCLs and the available control algorithms is provided.

2.2 DR with Aggregated TCLs

Due to limited capacity of individual consumers, they are not suitable to participate in frequency control service provision. Another problem is that the number of responsive appliances is so large that it is very difficult for the system operator to handle all these devices. Hence, aggregation of loads is an alternative for alleviating the complexity of too many devices participating in DR programs. In an MG, these aggregators act as an interface between the MGCC and consumers. TCLs are of the most appropriate candidates for frequency control service. Most common TCLs are air conditioner (A/C)s, heating ventilation and air conditioning (HVAC) systems, heat pumps,electric water heater (EWH), and refrigerator. TCLs can be controlled either by directly switching them on/off or indirectly by changing their temperature settings. A proper aggregation model for different types of loads can engage them in frequency regulation service. Due to the fact that TCLs can be properly controlled while providing acceptable comfort level to the costumers, and their fast acting properties, they can be considered as promising choices for ancillary services.

The main trade-off in problem of frequency control via DR programs is to maximize the comfort-level on the demand side, and minimize the participation of generation reserves and maximize the aggregated load curtailment duration on the utility side [4]. With integration of renewable energy resources, it is anticipated that more fluctuations will be added to the power balance in current power systems. In order to alleviate these unbalancing conditions, a large number of TCLs must be aggregated to provide the balance back to the system when any disturbance or intermittency occurs in the system. How to model these demands and how to control them via a reliable controller are two main questions which should be addressed. One approach is to consider smart appliances within every TCLA as individual responsive loads to the frequency deviation [15]. In this method, when the frequency goes above/below a threshold, the TCL is eligible to be turned on/off. However, if all the TCLs are turned on/off simultaneously, the frequency oscilation problem can occur [15]. As a solution to this problem, the participating TCLs can be chosen randomly. However, in this method the temperature and comfort level of the consumers are not taken into consideration. One parameter regarding the comfort level is to consider the minimum off(on)-time of the TCLs contributing in frequency control service [4]. If the frequency goes beyond a certain threshold, the load controller activates the participating aggregated loads, but these appliances which are turned off (on) must remain in the status for a specific period. For each single load, a Δf-τ control characteristic is desired: every appliance should turn on/off if the frequency deviation (Δf) goes above/below a controlling region, and its status must stay the same for a certain amount of time (τ). For simplicity, a common Δf-τ control characteristic is desired

for aggregation of a large number of appliances instead. This frequency-time characteristic helps the load controller in decision-making process. However, calculating the exact time for each appliance to take part in the service and the temperature dependency of the loads are not considered for most cases in the existing literature. Moreover, more complex systems which integrate renewable energy can make the Δf-τ characteristic more difficult to select. TCLs can be aggregated and controlled via their temperature settings. Hence, more detailed aggregation comes with consideration of temperature and dynamic characteristics of the TCLs [16]. For instance, in cooling systems, if the temperature setting is increased/decreased by a certain degree, TCLs can be turned off/on by load controller right away until the frequency deviation is cleared. The same method is applicable for EWHs. The advantage of temperature dependent frequency control with TCLs is that they can respond quickly to the setpoint signals in both primary and secondary control services. The drawback is that a number of devices will turn on/off simultaneously, which can lead to the frequency oscillation problem. To overcome the frequency oscillation problem and to improve the comfort level of the consumers, one approach is to let TCLs participate in the frequency regulation service via a priority list method [17]. An aggregation model can be applied by grouping TCLs into several clusters and listing these groups in a priority order, to provide the frequency control. According to the preceding discussion, an aggregated model based on the temperature settings, while accounting for comfort-level of consumers, is required.

2.3 Demand response control algorithms

In order to implement the DR programs, two main types of algorithms have been studied so far: centralized and decentralized control algorithms [18–20]. In centralized control, an upper level control center provides the control signals based on received data from measurement units distributed all over the system. Using communication links, these control signals are sent to the DR appliances to take part in the frequency control service. Nevertheless, in decentralized control, control signals are generated locally through local measuring and decision-making units with less complicated communication links [21]. These two types of algorithms are reviewed in more details in the following subsections.

2.3.1 Centralized control algorithms

The centralized approach is utilized for hierarchical models where a central controller sends proper operating signals from top to the lower level entities. Hence, a reliable communication link is necessary to connect the devices in different layers of the system to the central controller. Other important feature of the central controller is that it has a single point-of-failure. Due to simplicity of applications in DR programs, centralized algorithms have been investigated in many existing works, to control the frequency within an acceptable range. A central DR algorithm is proposed in [22] to stabilize the power system frequency while minimizing the curtailed load. In this method, when an unbalance occurs, frequency deviation will be brought within the acceptable range via an adaptive hill climbing (AHP) method. Different from [22]

where only DR is utilized to compensate for the unbalance of generation and load, a central control strategy is proposed where the frequency is regulated via both emergency DR (EDR) and slower generation reserve [23]. The EDR can be divided into two parts: The first part is to intercept the frequency decline and prevent from the load shedding; The second part is to bring the declined frequency back to a secure level, so that the slower responsive reserve can carry on the restoration afterwards to eliminate frequency steady state errors, and keep the frequency as close to the nominal as possible. The mentioned algorithms are simple and work well, however, it is important to take into account the cost of required communication links and the huge amount of data regarding the responrespectivesive appliances.

2.3.2 Decentralized control algorithms

The decentralized active DR (DADR) system is based on the assurance of power system unload services by multiple device actions without communication between individual elements [24]. The signal for load reduction is provided by the proposed control algorithm on the basis of frequency fluctuation measurements taken at the connection point of a DADR controlled device. Indeed, decentralized control strategies are based on local measurement and decision-making units. As moving forward in improving measurement technologies, these algorithms can be considered as promising DR control algorithms due to fast acting behavior and no required communication links. Numerous recent studies have discussed ferquency control via decentralized DR algorithms. To prevent the problem of dealing with a large number of DR appliances, decentralized controllers can take advantage of aggregated DR

providers. In [4], individual controllers for three types of loads (i.e. space heating loads, fridge/freezers, and storage water heaters) are considered aggregately to perform the primary frequency regulation. The aggregation characteristics of the individual loads determine the profile and global behavior of the demand-side reserve. Simulation results show a droop characteristic similar to a generator's primary frequency characteristic, suggests that DR can be potential resource for primary frequency control. In the abscence of two-way communication, the demand can respond to the frequency error in a manner similar to the generators. Decentralized control can also be performed by means of multi-agent control. For instance, in [25] a multi-agent demand control system is presented in which residential demand supports both primary and secondary frequency regulation. Again, loads are clustered and the aggregator of dynamic demand is able to control the power consumption and loads' response to frequency changes. The multi-agent control algorithm consists of two parts: one is to control the cluster of loads in real-time to obtain the planned consumption and the other is to plan the consumption of the cluster of loads over a time horizon. It is shown that, with the multi-agent control framework, the primary and secondary frequency control by a conventional generator can be imitated. Another approach in decentralized control is to let contracted consumers contribute to DR in a random manner which can be implemented for TCLs [15, 26].

2.3.3 Centralized vs. decentralized demand response control algorithms

In many cases, centralized control is not appropriate for primary frequency control. This is because the required reaction time for centralized DR services reaction, is often more than the frequency drop arresting time (which is normally up to a few seconds) [27–29]. The main reason for the latency relates to the required time of transferring information from DR appliances to the central controller and vice versa. However, decentralized control methods can provide a high dynamic response because they are capable of decision-making locally without time delay. It is demonstrated that these decisions can be executed without communication links in control centers, but based on the frequency measurements taken by each of the DADR devices at the load connection point [30]. For frequency control in small scale systems such as MGs, because the links are limitted with respect to large-scale ones, central control system can be a proper candidate. However, using hierarchial approach can reduce the communication cost even for these systems. The hybrid hierarchical control method is a combination of both centralized and decentralized methods, which can overcome the limitations of both methods [31]. A hybrid algorithm has significant advantages, e.g., reducing communication cost and delays significantly, and applicability for both primary and secondary control problems; however it is considered to be very complex in practical situations.

2.4 Summary

The problem of frequency control has been thoroughly discussed in literature. One of the main load types contributing to DR services is TCLs which have a high potential to take part in the frequency control services. Existing research show that they can participate in both primary and secondary frequency control due to their fast acting characteristics. However, providing appropriate aggregation models needs to be investigated in more depth. Current models regarding TCLs need to address thermal dynamic behaviors of TCLs to keep the comfort level of consumers as high as possible. The aggregated load models are controlled mainly by centralized and decentralized control algorithms for frequency control purposes. Centralized control is a simpler approach but requires to process a high amount of information which complicates the system, and is time consuming for controlling large scale systems which makes it suitable for the secondary control of such cases. Decentralized control is a better option for primary control due to its fast acting characteristics. The other advantage of decentralized control is no need for a complex and vast communication infrastructure which is essential for central controller. However, implementing decentralized approach is much more complex than centralized control. A hybrid hierarchical model which combines both centralized and decentralized models for the frequency control can be a choice.

Chapter 3

Aggregation TCL Model and Frequency Regulation

3.1 System Model

An MG can operate in both islanded and grid-connected mode through the PCC. MGs are also able to transit between these two operation modes. There exist MGs which are far from the main grid and cannot run in the grid-connected mode. MGs in remote communities or industrial sites are an example of this type. The frequency of the grid-connected MG is controlled by the main grid. However, in the islanded mode of operation, DERs and controllable loads can fulfill the frequency control of the MG. Due to their thermal inertia, TCLs can be regarded as one of the main types of controllable loads which can participate in a frequency regulation program. In order to investigate the frequency control by TCLs in MGs, we assume that the MG

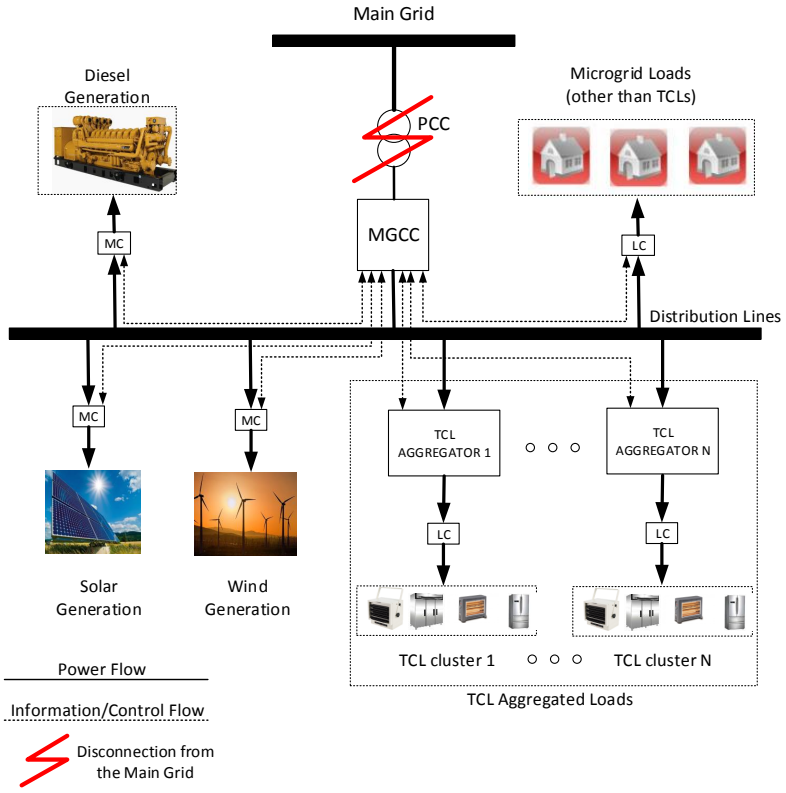

Figure 3.1: The system architecture of the MG.

under consideration operates in the islanded mode. The islanded MG is depicted in Figure 3.1, where the micro-source controllers (MC)s of DERs, load controller (LC)s of controllable loads, and the MGCC are in charge of controlling the frequency to maintain the supply-demand balance. On the supply side, the MG is equipped with synchronous/asynchronous generators such as DZ, WTs, and inverter-based generators (e.g., solar photo-voltaic (PV) panels).

On the demand side, the electric demand can be classified into controllable and non-controllable loads. The non-controllable loads such as lighting cannot participate in

the frequency regulation, while controllable loads such as TCLs can change their power consumption to control the frequency level. However, an individual TCL cannot significantly affect the frequency level of the islanded MG, due to its limited output power. In this regard, TCLs are aggregated to have noticeable impact on frequency of the system. Moreover, due to limited access of the MGCC to every contributing TCL in the MG, the approach of load aggregation is considered in our work [9–11]. In the following, each component of the system under consideration is further discussed in details.

3.1.1 Supply side model

The supply model includes renewable and non-renewable generation units. Based on characteristics of renewable energy resources, they usually do not participate in the frequency regulation. However, the synchronous generators can change their output power to control the frequency level of islanded MG. In this regard, synchronous generators are discussed more in detail here [32]. In order to have a good understanding of synchronous generator behaviours in frequency control, an important function which is called swing equation and its elements should be discussed. An important parameter in a synchronous machine is the power or load angle, $\delta(t)$, which is the time-varying angle between the position of the rotor axis and the magnetic field axis. When a disturbance occurs in the system, an oscillation occurs accordingly in which the rotor accelerates or decelerates depending on the load angle changes with respect to the rotating air gap magneto-motive force. This procedure is described by the following swing equation in the time domain, which is the basis for the frequency

control action of synchronous generators in power system stability analysis:

$$2H\frac{d^2\delta(t)}{dt^2} = P_m(t) - P_e(t). \tag{3.1}$$

In (3.1), ω_s is the electrical angular velocity, $P_m(t)$ is the driving mechanical power at time t, $P_e(t)$ is the electrical power output by the generator, and H is per unit inertia constant. With system frequency $\omega(t)=\frac{d\delta(t)}{dt}$, during a small perturbation denoted by Δ, the Laplace transform corresponding to (3.1) can be represented as $\Delta\omega(s) = \frac{1}{2Hs}[\Delta P_m(s) - \Delta P_e(s)]$, where s is Laplace transform operator. There are two types of loads fed by a synchronous generator, sensitive and non-sensitive to frequency. Frequency non-sensitive loads such as pure resistive loads are not dependent on frequency, and ideally any change in frequency has no impact on their behaviors. However, frequency dependent loads such as induction motors are affected by changes in frequency. As a result, a general load model can be represented as $\Delta P_e(s) = \Delta P_L(s) + D\Delta\omega(s)$, where $\Delta P_L(s)$ is the non-sensitive load, $D\Delta\omega(s)$ is the frequency dependent load, and D is the load damping constant indicating the percentage of change in the load with respect to 1% of the change in system frequency. Integrating the load formula with synchronous generator formula yields the block diagram of Figure 3.2. Two main elements of a synchronous machine are turbine and governor which produce and control mechanical power of the machine, respectively.

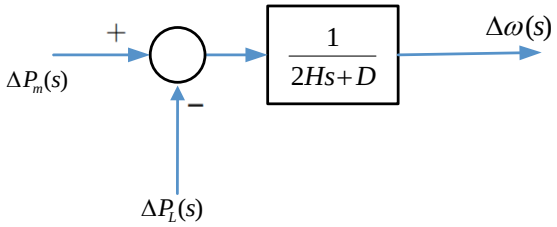

Figure 3.2: Generator-load model in Laplace transform.

Turbine and governor

A turbine is in charge of providing mechanical power which is a result of changes in the valve position of turbine. Figure 3.3 shows the model of a non-reheat steam turbine, where $\Delta P_V(s)$ represents the Laplace transform of changes in the valve position, τ_T is a time constant to model the mechanical delay of the turbine response to changes in valve position. The valve position is adjusted by the governor, which consequently results in adjustment of the mechanical output power of the turbine.

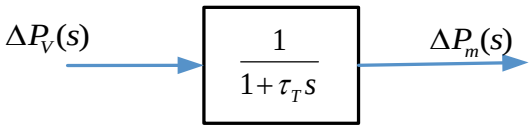

Figure 3.3: Modeling of a non-reheat steam turbine in Laplace transform.

The governor performs the power adjustment in accordance with changes in system frequency. In frequency control mode, the synchronous generator changes its generation using the governor based on the droop theory. Figure 3.4 provides an illustration of the droop theory. The slope of the droop control shows the characteristics of speed

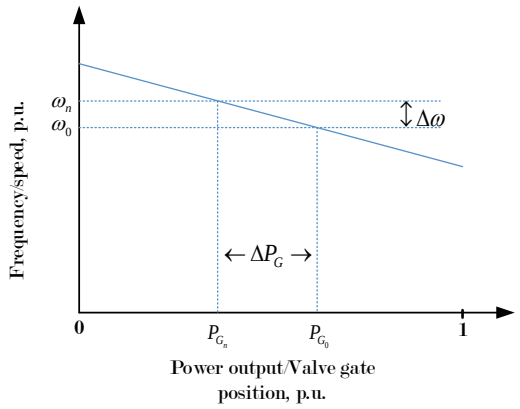

Figure 3.4: Droop characteristics of the governor.

regulation or droop R in (Hz/kW). It denotes the ratio of frequency deviation from the nominal value to the change in power output. The speed droop for generation units can be defined as

$$R\% = \frac{\Delta\omega}{\Delta P_G} \times 100 \tag{3.2}$$

where ω_n/P_{G_n} and ω_0/P_{G_0} are the rated and full-load frequency/power magnitude of the synchronous generator in $(rad/s)/kW$, respectively. According to the droop theory, decreasing/increasing frequency results in opening/closing the valve of the governor to increase/decrease the mechanical output of the turbine which is the input to the generator. Changes in input mechanical power of the generator causes changes in its output electrical power, which directly affects the system frequency. This can be shown in Laplace form of $\Delta P_g(s) = \Delta P_{ref}(s) - \frac{1}{R}\Delta\omega(s)$, where $\Delta P_{ref}(s)$ is the reference value of the generator and $\Delta P_g(s)$ is the deviation from the reference power which is a matter of changes in system frequency. The governor then changes the turbine valve position $\Delta P_V(s)$ with a specific time delay τ_g, resulting the modeling

in Figure 3.5.

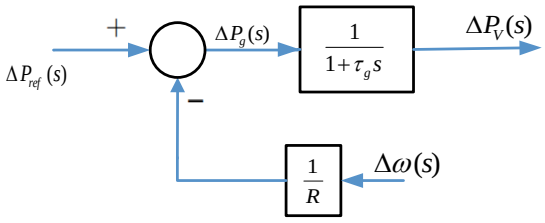

Figure 3.5: Modeling of a speed governor in Laplace transform.

The synchronous machine frequency control system can now be derived as shown in Figure 3.6, which is a combination of generator-load system, turbine and the governor block diagrams. Assuming the load change is a step input with magnitude ΔP_L, i.e., $\Delta P_L(s) = \dfrac{\Delta P_L}{s}$, the frequency deviation for a system of n generators in steady state can be derived using the Laplace final-value theorem, given by

$$\Delta\omega_{ss} = (-\Delta P_L)\frac{1}{D + \dfrac{1}{R_1} + \dfrac{1}{R_2} + ... + \dfrac{1}{R_n}} = \frac{-\Delta P_L}{\beta}. \tag{3.3}$$

In (3.3), the steady state frequency deviation of the system ($\Delta\omega_{ss}$) depends on the governor droop controllers in the system, where $\beta = D + \dfrac{1}{R_1} + \dfrac{1}{R_2} + ... + \dfrac{1}{R_n}$ represents the system frequency response characteristic. The droop control of governors is usually considered as the primary control, which acts within seconds to minutes to arrest the frequency drop as soon as possible. However, as shown in (3.3), implementing only the primary control will result in a steady-state frequency deviation from the desired value, depending on $R's$ and D parameters. Hence, secondary control is needed to bring the frequency back to its nominal value. In this regard, another block

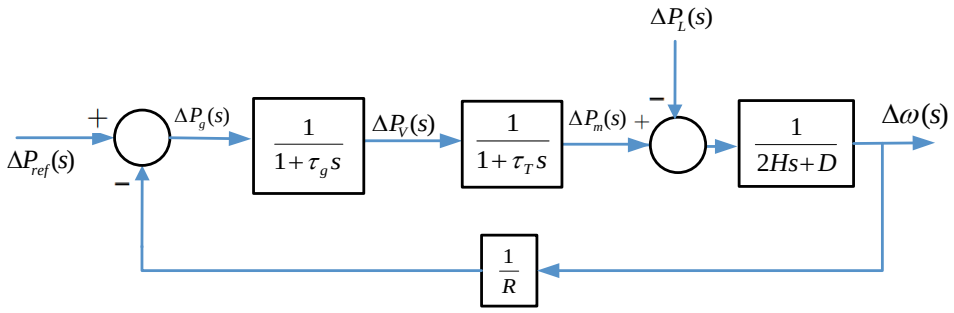

Figure 3.6: Modeling of a synchronous frequency control system with droop control in Laplace transform.

is added to the system which represents the secondary control in Laplace form of $\frac{K_I}{s}$, with the secondary frequency control integrator gain K_I. The secondary control action basically adjusts the load reference set-point of governor. The modeling of synchronous machine frequency control system with primary and secondary control in Laplace transform is illustrated in Figure 3.7, where both control modes are used to adjust the mechanical power based on changes in system frequency.

3.1.2 Demand side model

Controllable loads participating in frequency control include mainly heating, ventilation, air conditioners, electric water heaters and cooling devices such as refrigerators, which are called TCLs. All the information regarding these loads is measured using smart meters in the MG, and is sent to the TCLAs. Aggregators have two-way communication with the MGCC, and are responsible to allocate power to DR par-

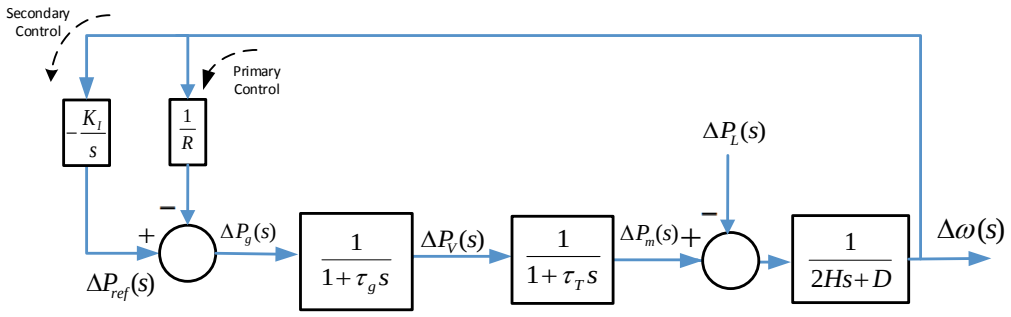

Figure 3.7: Modeling of a synchronous frequency control system with primary and secondary control in Laplace transform.

ticipants. TCLAs are prioritized according to their availability and the consumer level of comfort. Here, the control process of TCL output power in response to frequency deviations is called demand response (DR). The diagram of the aggregating N TCLAs is provided in Figure 3.8, As can be seen in this figure, power from all TCLs are aggregated within TCLAs to form the total power from DR (P_{DR}).

DR of TCLs must take into account their dynamic behavior of temperature, physical limitation in the operating states (on/off), and their nature of distribution. The thermal dynamics of an individual TCL is the fundamental of developing the aggregation model and control scheme. TCL modelling is commonly represented in two forms of first order and second order differential equations. For instance, in an air-conditioned room, the heat flow between room air and outside air is modeled by a first-order differential equation, whereas an added consideration of the heat exchange between room air and room furnishing requires a second-order differential equation. For simplicity, we consider the popular first-order equivalent thermal parameter (ETP) model [33]. In this model, the internal dynamics of conditioned mass

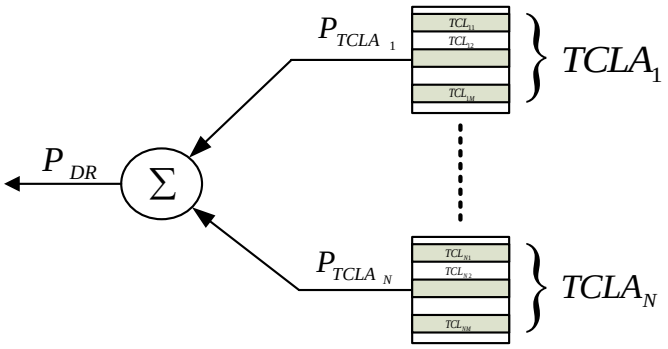

Figure 3.8: Block diagram of aggregating N TCLAs.

of the thermal system (ignoring the impact of the building mass temperature) are considered to represent individual TCL dynamic operation. This method is suitable for residential or small commercial buildings to describe the dynamics of individual loads. In this model, both the ambient temperature and heating flux affect the indoor temperature. The equivalent electric circuit of the ETP model is illustrated in Figure 3.9. The dynamics can be described by

$$\dot{\theta}_{in}(t) = \frac{1}{CR}(\theta_a(t) - \theta_{in}(t) - RP_r(t)) \tag{3.4}$$

where $\theta_{in}(t)$ and $\theta_a(t)$ are the indoor and ambient air temperature at time t respectively, $C[kWh/^\circ C]$ is the thermal capacitance connected in series with a thermal resistance $R[^\circ C/kW]$, and $P_r(t)$ is the equivalent heat rate at time t. The physical parameters of individual TCLs include thermal resistance, capacitance, and active power consumption.

Since we have a large number of different individual TCLs in the MG, it is nec-

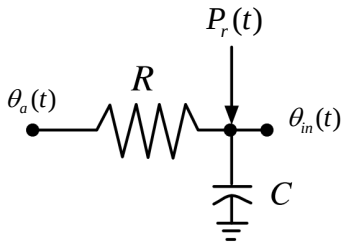

Figure 3.9: First-order ETP model [31].

essary to consider the heterogeneity of TCLs in our model. We group heterogeneous TCLs into N homogeneous classes according to their physical parameters. Each class is controlled by an aggregator (i.e., TCLA) which manages the homogeneous cluster of TCLs. Aggregation of power from all the TCLAs results in P_{DR}. DR performs similarly to spinning reserve in magnitude and power flow direction. That is, once frequency deviation is negative (positive), it is required to turn off (on) a portion of the responsive loads. For small perturbations, the general system equation for the purpose of MG frequency control analysis including DR and renewable energy resources is given in Laplace form by [34]

$$\Delta P_{Non-Ren}(s) + \Delta P_{Ren}(s) + \Delta P_{DR}(s) - \Delta P_L(s) = 2Hs\Delta\omega(s) + D\Delta\omega(s) \quad (3.5)$$

where $\Delta P_{Non-Ren}(s)$ is the power from non-renewable units such as DZ, $\Delta P_{Ren}(s)$ is the power from renewable energy units, $\Delta P_{DR}(s)$ is the power from DR, $\Delta P_L(s)$ is the load perturbation, $\Delta P_{Non-Ren}(s) + \Delta P_{Ren}(s) + \Delta P_{DR}(s) - \Delta P_L(S)$ represents the power mismatch, and $\Delta\omega(s)$ is the frequency deviation.

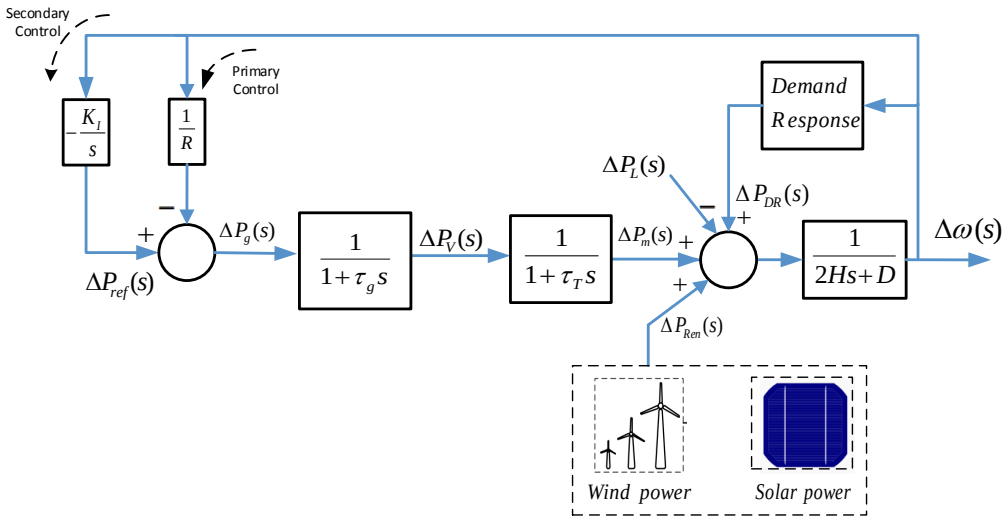

Figure 3.10: Modeling of supply side including synchronous generator and renewable energy in presence of responsive demands in Laplace transform.

Integrating the synchronous generator model, together with renewable energy resources blocks such as PV generation and a wind turbine as well as the feedback loop for DR, results in Laplace transform model in Figure 3.10. The parameters of the synchronous generation system block are assumed to be the equivalent of all generation assets and load damping of the MG.

3.2 Research Problem

The research objective is to aggregate and control TCLs in order to maintain the frequency level of an islanded MG, and to keep the comfort level of the costumers in a desired range, subject to renewable energy/load changes in the MG. The TCL

aggregation model aims to obtain a fast response to load changes or renewable intermittency to regulate the frequency in a specific operating range. Furthermore, this aggregation process is to maintain comfort level of customers while keeping TCLs' temperature in a desired range.

In the islanded MG, load changes and intermittent behaviors of renewable energy resources cause system frequency to deviate from its nominal value. The frequency control system should keep the frequency of the MG within its acceptable operating range. This should be done by properly incorporating the TCLs in the frequency control. Minimizing frequency deviation due to load perturbations/renewable energy intermittency in the MG is done by applying DR with the TCL aggregation model. Due to small impact of an individual TCL on MG control, it is necessary to engage a large number of TCLs into frequency regulation. The problem becomes complex because not only we deal with a large number of devices, but also we need to ensure the customers' comfort level.

Given limitations of existing TCL aggregation models as discussed in Chapter 2, our objective is to design a TCL aggregation strategy for MG frequency control purposes. Under this aggregation method, heterogeneous TCLs are grouped into several classes. TCLAs are responsible to manage each group of TCLs, and TCLs are prioritized based on their setting temperature statuses. These aggregators have two-way communication with MGCC, and LCs are in charge of controlling the TCLs locally. Aggregated TCLs are controlled via changing the temperature settings by TCLAs. As soon as a noticeable drop/increase in frequency is sensed via meters in the MG, the MGCC calculates the required power and cooperates with aggregators to switch

TCLs off/on as needed. In order to have a proper aggregation and control scheme of TCLs for the frequency regulation, the following research issues are studied:

1. Controlling an individual TCL is less challenging than controlling a large number of TCLs. The main challenge of frequency control via controlable loads is the large number of potential participants, and difficulties in dealing with many small loads rather than a limited number of generating units. In particular, the cost and complexity associated with two-way communications between many loads and the MGCC can be overwhelming obstacles [4]. This also leads to the fact that, when the number of TCLs increases, their heterogeneity increases as well. Hence, aggregating a large number of heterogeneous TCLs becomes challenging and an aggregation model is required to account for their heterogeneity [9–11]. To address both the large number and heterogeneity of TCLs, one approach is to group TCLs into several TCL clusters. In this structure, the MGCC communicates with aggregators of clusters as represented in Figure 3.1 instead of a single aggregator for a large number of TCLs. In our study we apply the aggregation model proposed in [12] as a basis to take advantage of TCLs for fast frequency regulation purposes.

2. The frequency oscillation problem, which occurs when smart appliances simultaneously respond to the system frequency by varying their power consumption, is the main barrier to realize DR-enabled frequency control in practice [15]. In a case of frequency drop, turning off a large number of TCLs can take the frequency out of its desired range. Moreover, if TCLs are switched on/off with

no limitation, the life-cycle of these devices will be reduced. Hence, in order to prevent the frequency oscillation problem, frequent switching actions and avoiding the chance of running out of the desired range of frequency, minimum on/off time of TCLs is considered in our model.

3. In conventional frequency control problems, the regulation of frequency is acheived solely from the generation side. However, by enabling the demand side (i.e. TCLs contributing into frequency control), a challenge is to deal with the coordination among the frequency regulation providers. In this regard, it is required that aggregated TCLs provide frequency control in accordance with synchronous generation of the system. The problem should be solved by considering both power system dynamics and thermodynamics of the system. The MGCC should be responsible to provide this coordination such that changes in system load and intermittency of the renewable energy resources imposed to the system are compensated.

The contributions of this study includes prioritizing the TCLAs instead of individual TCLs, which takes into account the thermal dependability of TCLs within aggregation model. Also, aggregation models such as the one in [12] have been mainly used for load following purposes and the relative case studies are in a time scale of minutes to several hours. To the best of the our knowledge, this study is one of the very few studies which deal with fast regulation performed by aggregated TCLs in islanded MGs in order of seconds. Moreover, we consider the coordination of generation (renewable-non-renewable) and DR in an islanded MG instead of sim-

ply using the load-supply balancing signal from the power system operator. We also consider the lockout effect of individual TCLs to make the model more cost efficient and reliable.

3.3 TCL Aggregation Model for Frequency Regulation

TCLs are potential candidates to support frequency regulation in the MG. In order to regulate frequency with TCLs, it is important to have proper modeling of both individual and aggregated TCLs. This is because a large number of heterogeneous TCLs exist in MGs, and desirable aggregation and control of these loads are crucial to provide the regulation service. In the aggregation and control of TCLs, the first order TCL modeling is considered for simplicity. In the following, electric/thermal formulations of individual and aggregated TCLs for frequency regulation is presented [11,35].

3.3.1 Individual TCL Model

A TCL can be modeled as a thermal capacitance, $C_i[kWh/^\circ C]$, connected in series with a thermal resistance, $R_i[^\circ C/kW]$, where i is index of the i^{th} TCL [11, 36]. The dynamic behavior of TCL can be modeled by two state variables, the discrete operation state $s_i(t)$, and the internal temperature $\theta_i(t)$ of the conditioned mass (i.e., indoor air temperature) as in (3.6), where $s_i(t) = 1$ indicates TCL i is on, and $s_i(t) = 0$ represents TCL i is turned off at time t. The TCL hybrid state model can be represented by n_k first-order ordinary differential equations

$$\dot{\theta}_i(t) = \frac{1}{C_i R_i}(\theta_{a,i}(t) - \theta_i(t) - s_i(t) R_i P_{r,i}), \qquad i = 1, 2, ..., n_k \tag{3.6}$$

where $P_{r,i}[kW]$ is the constant electrical consumption, $\theta_{a,i}$ represents the ambient temperature (i.e., outdoor air temperature of a building), and N_L is the number of TCLs within an aggregator. In general, a negative sign in $P_{r,i}[kW]$ means a heating TCL and positive sign refers to a cooling TCL. In this study, we consider only cooling devices, hence $P_{r,i}[kW]$ is nonnegative. Similar approach can be used for heating devices with a negative value for $P_{r,i}[kW]$. In our study, we do not consider the thermal noise (e.g., effects of opening doors and windows).

In (3.6), the binary dimensionless functions $s_i(t)$ is the operation state governed by a thermostatic switching law to keep the temperature of a TCL within a predetermined temperature deadband, given by

$$s_i(t) = \begin{cases} 0, & if\ s_i(t-\tau) = 1 \quad \& \quad \theta_i(t) < \theta_i^- \\ 1, & if\ s_i(t-\tau) = 0 \quad \& \quad \theta_i(t) > \theta_i^+ \\ s_i(t-\tau), & Otherwise \end{cases} \tag{3.7}$$

where τ is the sampling period, θ_i^- and θ_i^+ are the lower and upper limit of the temperature deadband $\Delta_{db,i}$ around the setting temperature $\theta_{set,i}$ for i^{th} TCL given by

$$\theta_i^- = \theta_{set,i} - \Delta_{db,i}, \quad \theta_i^+ = \theta_{set,i} + \Delta_{db,i}. \tag{3.8}$$

We consider the setpoint temperature $\theta_{set,i}$ as the control input for each TCL. Considering the fact that different consumers have different comfort levels, the control input should satisfy

$$\theta_{set,i}^- < \theta_{set,i} < \theta_{set,i}^+ \tag{3.9}$$

where $\theta^{-}_{set,i}$ and $\theta^{+}_{set,i}$ are the lower and upper bounds of the i_{th} customer's acceptable regulation thresholds.

An illustration of a TCL operation in a cooling scenario is provided in Figure 3.11. When the TCL is turned on, the temperature of the conditioned mass decreases, until reaching the lower threshold θ^{-}_{i}. In this case, the TCL will automatically turn off. By turning off the TCL, the temperature will increase until it reaches the higher threshold θ^{+}_{i}. At this point, the TCL is turned on, and the cycle continues. This type of control is designed such that the comfort level of the costumers is respected.

Lockout effect of TCLs: In real applications, in order to protect the appliance from

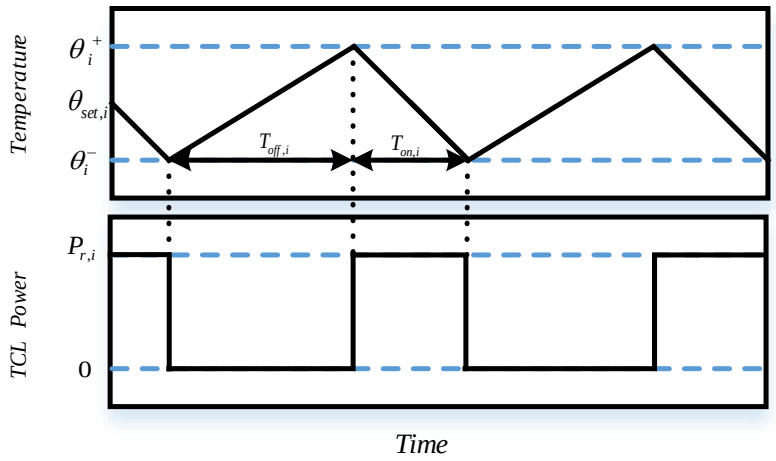

Figure 3.11: Dynamics of a TCL (cooling scenario).

continuously switching between on and off statuses, a minimum time is set as switch-

on/-off threshold. Once TCL starts running, it should not be turned off immediately, and when it is turned off, there is a minimum time before which it cannot be turned back on. Thus, in order to meet this constraint, the control process should be done according to the up-time and down-time of TCL. The lockout constraint of TCL can be expressed by

$$(T_{on,i}(t) - T_{up,i})(s_i(t-\tau) - s_i(t)) \geq 0 \tag{3.10a}$$

$$(T_{off,i}(t) - T_{down,i})(s_i(t) - s_i(t-\tau)) \geq 0 \tag{3.10b}$$

where $T_{on,i}(t)$ and $T_{off,i}(t)$ are the continuous on and off time of TCL i at time t, respectively; $T_{up,i}$ and $T_{down,i}$ denote the minimum up- and down-time of TCL i, respectively, stating a TCL unit must stay in the on status for a duration of at least $T_{up,i}$ from the time it is switched on, and it must stay in the off status for a duration of at least $T_{down,i}$ from the time it is switched off. When switching TCLs on/off at a certain time instant t, the constraints of (3.10) should be considered.

3.3.2 TCL Aggregation Model

Due to small impact of an individual TCL on MG control, it is necessary to engage a large number of TCLs into frequency regulation. In order to aggregate TCLs in an islanded MG, we cluster the population of heterogeneous TCLs into several homogeneous clusters which are handled by a number of TCLAs. Heterogeneous TCLs are clustered based on parameters in Table 3.1.

We partition the set of TCLs into clusters (controlled by aggregators), $\bigcup_{k=1}^{n_A} \Psi_k$,

Table 3.1: Clustering parameters for heterogeneous aggregated TCLs

Description	**Parameter**	**Unit**
Thermal resistance	R	$°C/kW$
Thermal capacitance	C	$kWh/°C$

where $k \in \{1, ..., n_A\}$, and n_A is the number of aggregators, and denote $\Psi_k = \{1, 2, ..., n_k\}$ where n_k is the number of TCLs in the k^{th} aggregator.

a. Basic TCL aggregation model

Let i_k denote the index of TCLs in aggregator k. In order to formulate the aggregation model of TCL $i_k \in \Psi_k$, the steady state cooling time T_{on,i_k} and the steady state heating time T_{off,i_k} for the i_k^{th} TCL can be calculated by solving (3.6), given by [37]

$$T_{on,i_k} = C_{i_k} R_{i_k} \ln\left(\frac{P_{r,i_k} R_{i_k} + \theta_{i_k}^{+} - \theta_{a,i_k}}{P_{r,i_k} R_{i_k} + \theta_{i_k}^{-} - \theta_{a,i_k}}\right), \qquad i \in \Psi_k \tag{3.11a}$$

$$T_{off,i_k} = C_{i_k} R_{i_k} \ln\left(\frac{\theta_{a,i_k} - \theta_{i_k}^{-}}{\theta_{a,i_k} - \theta_{i_k}^{+}}\right). \tag{3.11b}$$

Based on the steady state temperature on and off time of TCL $i_k \in \Psi_k$, the total average power consumption P_{TCL} of TCLs can be obtained as

$$P_{TCL} = \sum_{k=1}^{n_A} \sum_{i_k=1}^{n_k} \frac{T_{on,i_k} P_{r,i_k}/(\eta)}{T_{on,i_k} + T_{off,i_k}}, \qquad i_k \in \Psi_k. \tag{3.12}$$

In (3.12), normal operation of TCLs has freedoms to work between the lower and upper bound of temperature due to the finite values of T_{on,i_k} and T_{off,i_k}. The control variable in (3.7) can be used as an "external" command to switch the TCLs on or off. However, the required response can also be specified implicitly by mediating

the setpoint temperature levels. The option of regulating frequency by changing the temperature setpoints provides one way for TCLs to enforce individual temperature bound for each appliance to meet the service quality constraints. Therefore, with TCLs, we have the capability to regulate the frequency by turning them on/off when needed, while taking into account the comfort level of the costumers.

In practical situations, dynamic system of (3.12) is difficult to apply because this aggregation model needs a very high order system representing each TCL using a separate differential equation, which is difficult to analyze for the system operator. This is because the system operator must obtain the state of every TCL at all times, which is difficult in a large-scale aggregation system. Moreover, the temperature interdependency of TCLs is not considered in (3.12), and TCLs are switching on/off independently. Hence, an aggregation model addressing these issues is needed for the frequency regulation.

b. Transport TCL aggregation model

An aggregation model based on a set of partial differential equations (PDEs) is discussed, which governs the transport of TCL temperatures within their respective ranges according to the increase and decrease of temperatures [12]. In the following, the TCL transport model is discussed for a single aggregator which is a more comprehensive and faster method than that of (3.12), making it suitable for frequency regulation applications.

For a large population of TCLs in a cooling scenario in every aggregator, we distribute them over the on and off states as shown in Figure 3.12 [12]. It is assumed that the entire TCL population is distributed in a finite temperature range $[\theta^{-}_{set},\ \theta^{+}_{set}]$.

Some of the loads are distributed over the on state to cool down towards the minimum dead-band temperature θ^-, while some other are distributed over the off state moving towards the maximum dead-band θ^+. TCLs migrate in the temperature deadband according to the on/off switching law as stated in (3.7). TCLs with temperatures hitting the deadband thresholds change their states from on to off and vice versa. This migration process can be described by two distinct transport processes with coupled boundary conditions for every aggregator as discussed next.

Let $X_{on}(t,\theta)$ and $X_{off}(t,\theta)$ denote the distribution of loads [number of loads/°C]

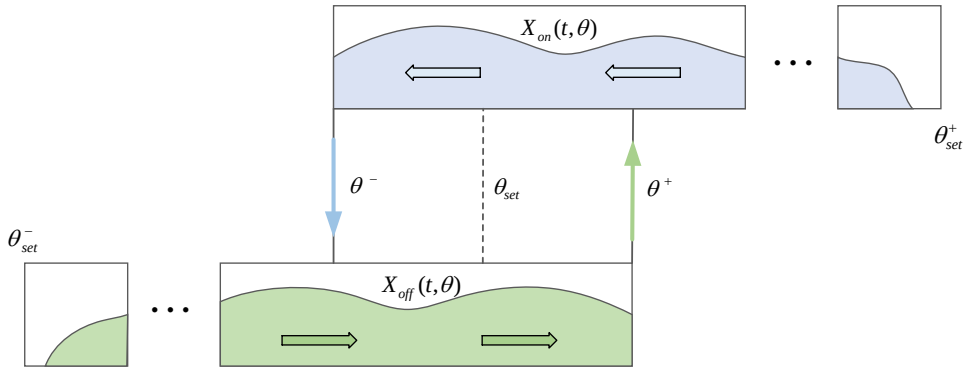

Figure 3.12: Aggregate TCL transport process [10].

at time t and temperature θ over the on and off states, respectively. Assuming parameter homogeneity for the studied aggregator, the flow of the loads [number of

loads/sec] crossing temperature θ at time t is equal to

$$F_{on/off}(t,\theta) = X_{on/off}(t,\theta)\left[\frac{\delta\theta}{\delta t}\right]_{on/off} \tag{3.13a}$$

$$X_{on}(t,\theta) = \sum_{i_k=1}^{n_k} s_{i_k}(t,\theta_{i_k}), \qquad \theta < \theta_{i_k} < \theta + \delta\theta \tag{3.13b}$$

$$X_{off}(t,\theta) = \sum_{i_k=1}^{n_k} (1 - s_{i_k}(t,\theta_{i_k})), \qquad \theta < \theta_{i_k} < \theta + \delta\theta \tag{3.13c}$$

where term $\frac{\delta\theta}{\delta t}$ denotes the change of TCL temperature in time, which can be obtained from (3.6). It is noteworthy to mention that $s_{i_k}(t)$ is determined with the consideration of lockout effect of i_k^{th} TCL as mentioned in (3.10). By substituting (3.6) into (3.13) one can obtain

$$F_{on}(t,\theta) = \frac{1}{CR}(\theta_a - \theta - RP)X_{on}(t,\theta) = \alpha_{on}(\theta_a,\theta)X_{on}(t,\theta) \tag{3.14a}$$

$$F_{off}(t,\theta) = \frac{1}{CR}(\theta_a - \theta)X_{off}(t,\theta) = \alpha_{off}(\theta_a,\theta)X_{off}(t,\theta) \tag{3.14b}$$

with α_{on} and α_{off} representing the TCL transport rates over the on and off states, respectively. In a constant ambient temperature, by neglecting the variation of temperature around the initial setpoint $\theta_{set,0}$, (3.14) can be rewritten to yield following approximated parameters [12]

$$\alpha_{on}(\theta_a,\theta) \approx \overline{\alpha}_{on}(\theta_a,\theta_{set,0}) = \frac{1}{CR}(\theta_a - \theta_{set,0} - RP) \tag{3.15a}$$

$$\alpha_{off}(\theta_a,\theta) \approx \overline{\alpha}_{off}(\theta_a,\theta_{set,0}) = \frac{1}{CR}(\theta_a - \theta_{set,0}). \tag{3.15b}$$

In 3.15, $\overline{\alpha}_{on}(\theta_a, \theta_{set,0})$ and $\overline{\alpha}_{off}(\theta_a, \theta_{set,0})$ correspond to the average rates of temperature drop and rise over the on and off states, respectively. In the remaining deviations, the exact expressions for α_{on} and α_{off} are used, and the approximate values are used for discritized approximation of the system.

Boundary condition: The rate of increase of the TCL concentration, for a small control volume of length $\delta\theta$, is calculated from the difference between the entering flux and the outgoing flux divided by the magnitude of the control volume as stated in (3.16). The process is shown in Figure (3.13), and is given by

$$\frac{\partial X_{on/off}(t,\theta)}{\partial t} = \lim_{\delta\theta \to 0} \frac{F_{on/off}(t,\theta) - F_{on/off}(t,\theta+\delta\theta)}{\delta\theta} = -\frac{\partial F_{on/off}(t,\theta)}{\partial\theta}. \quad (3.16)$$

By substituting (3.15) into (3.16), the governing PDE of the system can be obtained

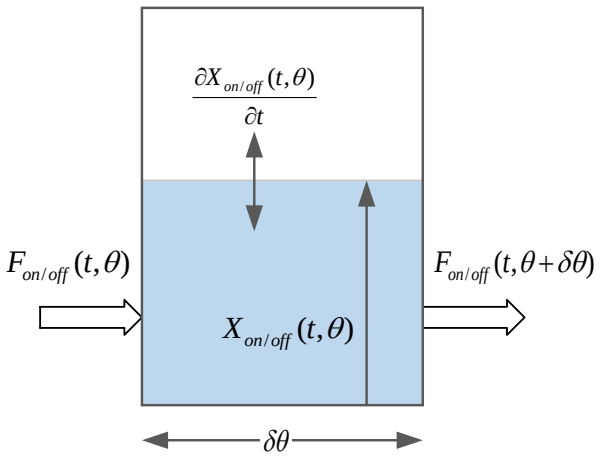

Figure 3.13: Effect of entering and outgoing flux on TCL numbers in the control volume [10].

by

$$\frac{\partial X_{on/off}(t,\theta)}{\partial t} = -\frac{\partial[\,\alpha_{on/off} X_{on/off}(t,\theta)]}{\partial \theta}. \tag{3.17}$$

Equation (3.17) yields two first-order linear transport processes coupled through the conservation of flux at the thermostat boundaries as follows

$$[\,\alpha_{on} X_{on}(t,\theta)]_{@\theta_l^+} - [\,\alpha_{on} X_{on}(t,\theta)]_{@\theta_u^+} + [\,\alpha_{off} X_{off}(t,\theta)]_{@\theta^+} = 0 \tag{3.18a}$$

$$[\,\alpha_{off} X_{off}(t,\theta)]_{@\theta_u^-} - [\,\alpha_{off} X_{off}(t,\theta)]_{@\theta_l^-} + [\,\alpha_{on} X_{on}(t,\theta)]_{@\theta^-} = 0. \tag{3.18b}$$

where l and u are indexes to show magnitudes lower/higher than but close to an specific temperature, respectively. Moreover, at the lower and higher bounds of the costumer's acceptable regulation thresholds, i.e., θ_{set}^- and θ_{set}^+,

$$\alpha_{off} X_{off}(t,\theta) = \alpha_{on} X_{on}(t,\theta) = 0. \tag{3.19}$$

It should be noted that $\theta \in [\,\theta^-,\ \theta_{set}^+]$ for $X_{on}(t,\theta)$, and $\theta \in [\theta_{set}^-,\ \theta^+]$ for $X_{off}(t,\theta)$. Equations (3.17)-(3.19) denote the dynamics of the system with a fixed temperature setpoint (θ_{set}). Next, we will discuss the system dynamics considering a varying temperature setpoint.

In the case of frequency regulation, it is required to change the temperature setting of TCLs to control their output power. Hence, a model to consider the setpoint variation of TCL temperature is needed. In this regard, the control volume is shifted along with the temperature setpoint variation in the transport TCL model as depicted in Figure 3.14. The flux which is seen by the fixed control volume minus

the flux induced by shifting the control volume due to temperature setting variation equals the total TCL flux seen by the moving control volume

$$\begin{aligned} F_{on}(t,\theta) &= X_{on}(t,\theta)\left[\frac{\delta\theta}{\delta t}\right]_{on} - X_{on}(t,\theta)\frac{\delta\theta_{set}}{\delta t} \\ &= X_{on}(t,\theta)(\alpha_{on} - \dot{\theta}_{set}(t)) \end{aligned} \tag{3.20a}$$

$$\begin{aligned} F_{off}(t,\theta) &= X_{off}(t,\theta)\left[\frac{\delta\theta}{\delta t}\right]_{off} - X_{off}(t,\theta)\frac{\delta\theta_{set}}{\delta t} \\ &= X_{off}(t,\theta)(\alpha_{off} - \dot{\theta}_{set}(t)). \end{aligned} \tag{3.20b}$$

We can now obtain the governing PDE of the TCL transport model, considering temperature setting variation

$$\frac{\partial X_{on/off}(t,\theta)}{\partial t} = -\frac{\partial[\,(\alpha_{on/off} - \dot{\theta}_{set}(t))X_{on/off}(t,\theta)]}{\partial\theta} \tag{3.21}$$

with thermostatic coupling conditions considering the temperature setting variation

$$\begin{aligned} &[\,(\alpha_{on} - \dot{\theta}_{set}(t))X_{on}(t,\theta)]_{@\theta_l^+} - [\,(\alpha_{on} - \dot{\theta}_{set}(t))X_{on}(t,\theta)]_{@\theta_u^+} \\ &+ [\,(\alpha_{off} - \dot{\theta}_{set}(t))X_{off}(t,\theta)]_{@\theta^+} = 0 \end{aligned} \tag{3.22a}$$

$$\begin{aligned} &[\,(\alpha_{off} - \dot{\theta}_{set}(t))X_{off}(t,\theta)]_{@\theta_u^-} - [\,(\alpha_{off} - \dot{\theta}_{set}(t))X_{off}(t,\theta)]_{@\theta_l^-} \\ &+ [\,(\alpha_{on} - \dot{\theta}_{set}(t))X_{on}(t,\theta)]_{@\theta^-} = 0. \end{aligned} \tag{3.22b}$$

Note that, if we set $\dot{\theta}_{set}(t) = 0$, we will obtain the same equations of (3.17)-(3.19). We assumed that setting temperature is varying in the range of $\left[\theta_{set}^-,\ \theta_{set}^+\right]$. Besides, we assume that all the TCL population of aggregator exists in this range. These

two assumptions guarantee the zero flux condition at the extreme temperatures, i.e., (3.19). In the next section, the temperature discritized model of the above-mentioned equations is investigated to provide a finite-dimensional state space model for the aggregation of TCLs.

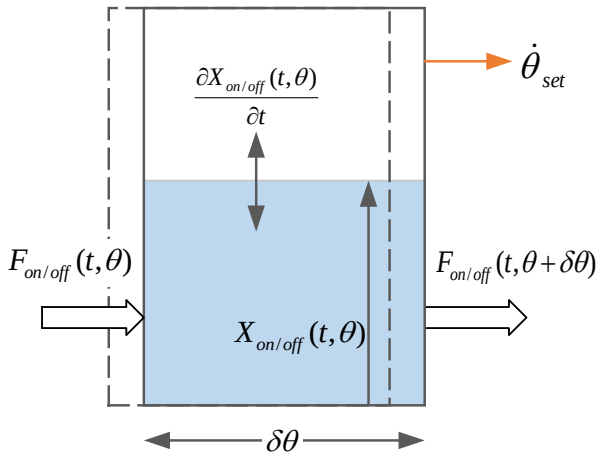

Figure 3.14: Moving state bin for varying setting temperature [10].

Finite-dimensional state space model: The temperature discritization of the transport PDEs aims to provide a finite-dimensional state space model for the aggregation of TCLs. In this method, the temperature range $\left[\theta_{set}^{-}, \theta_{set}^{+}\right]$ is divided into small bins with uniform lengths. For every bin, the difference between the entering and outgoing TCL flux leads to the variation of number of TCLs in that bin. The discritization is shown in Figure 3.15. After discretizing (3.21), considering the average values of the transport coefficients $\overline{\alpha}_{on}$ and $\overline{\alpha}_{off}$ the following state-space equations are

obtained [12]

$$\dot{x}_j(t) = \begin{cases} -\dfrac{\overline{\alpha}_{off} - \dot{\theta}_{set}(t)}{\Delta\theta}(x_j(t) - x_{j-1}(t)), & j = 2, 3, ..., M, M+2, ..., N \\ -\dfrac{\overline{\alpha}_{on} - \dot{\theta}_{set}(t)}{\Delta\theta}(x_{j+1}(t) - x_j(t)), & j = N+1, ..., P-1, P+1, ..., Q \end{cases} \tag{3.23}$$

where $x_j(t)$ represents the number of TCLs at bin j, and $\Delta\theta$ is the temperature discretization length. The arrangement of discritized bins with indexes M, N, P and Q is depicted in Figure 3.15. There are N bins for disctization of off state TCLs , and a total of Q bins for the whole temperature range (including on and off states). The conceptual meaning of (3.23) is to declare that the entering number of TCLs

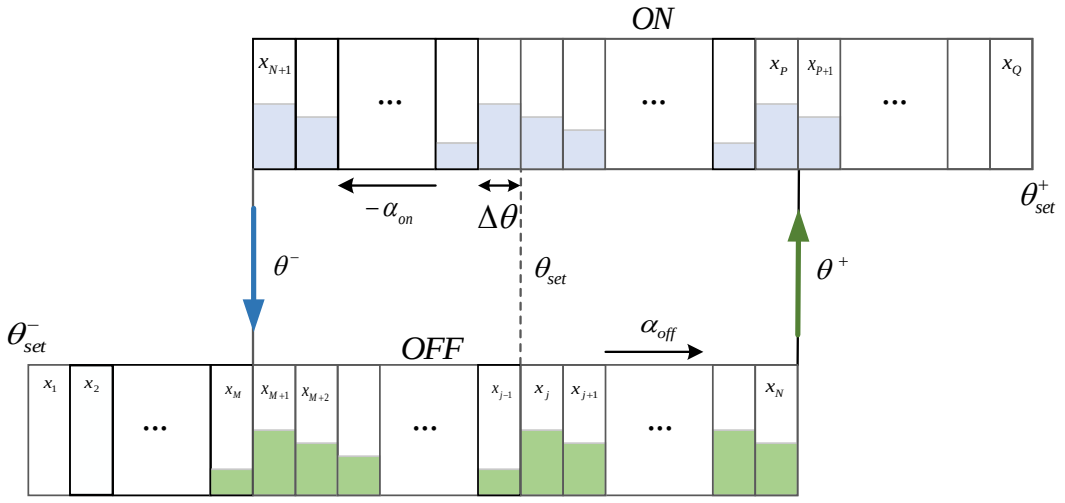

Figure 3.15: Finite-difference discritization of the temperature range to derive the state space model [10].

to a specific bin minus exiting ones yields the change rate of total number of TCLs in that bin. For the boundary bins, based on (3.23), we can obtain the following equations [12]

$$\begin{aligned}
\dot{x}_1(t) &= -\frac{\overline{\alpha}_{off} - \dot{\theta}_{set}(t)}{\Delta\theta} x_1(t) \\
\dot{x}_{M+1}(t) &= -\frac{\overline{\alpha}_{off} - \dot{\theta}_{set}(t)}{\Delta\theta}(x_{M+1}(t) - x_M(t)) - \frac{\overline{\alpha}_{on} - \dot{\theta}_{set}(t)}{\Delta\theta} x_{N+1}(t) \\
\dot{x}_P(t) &= -\frac{\overline{\alpha}_{on} - \dot{\theta}_{set}(t)}{\Delta\theta}(x_{P+1}(t) - x_P(t)) - \frac{\overline{\alpha}_{off} - \dot{\theta}_{set}(t)}{\Delta\theta} x_N(t) \\
\dot{x}_Q(t) &= -\frac{\overline{\alpha}_{on} - \dot{\theta}_{set}(t)}{\Delta\theta} x_Q(t).
\end{aligned} \tag{3.24}$$

Now we can calculate the aggregated TCL power by multiplying the summation of loads over the on state by consuming power of each TCL

$$P_{TCL}(t) = \frac{P}{\eta} \sum_{j=N+1}^{Q} x_j(t). \tag{3.25}$$

A standard bilinear state-space matrix representation of the aggregation system can be obtanined by equations (3.23)-(3.25), given by

$$\begin{aligned}
\dot{x}(t) &= Ax(t) + Bx(t)u(t), \;\; u(t) = \dot{\theta}_{set}(t) \\
y(t) &= Cx(t)
\end{aligned} \tag{3.26}$$

where $x(t) = [x_1(t), x_2(t), ..., x_Q(t)]^T$ is the $Q \times 1$ state vector, $y(t) = P_{TCL}(t)$ is the aggregate TCL power, $C = [\underbrace{0, ..., 0}_{N}, \underbrace{P/\eta, ..., P/\eta}_{Q-N}]$ is the $1 \times Q$ state to output vector, A is the $Q \times Q$ state matrix and B is the $Q \times Q$ input matrix. These matrices are

given in (3.27) and (3.28), as follows: .

$$A = \left[\begin{array}{cc|c} -\overline{\alpha}_{off} & & \\ \overline{\alpha}_{off} & -\overline{\alpha}_{off} & \\ \ddots & \ddots & \\ \hline & \overline{\alpha}_{off} \; -\overline{\alpha}_{off} & -\overline{\alpha}_{on} \\ & \ddots \quad \ddots & \\ & \overline{\alpha}_{off} \; -\overline{\alpha}_{off} & \\ \hline & & \overline{\alpha}_{on} \; -\overline{\alpha}_{on} \\ & & \ddots \quad \ddots \\ & \overline{\alpha}_{off} & \overline{\alpha}_{on} \; -\overline{\alpha}_{on} \\ \hline & & \ddots \quad \ddots \\ & & \overline{\alpha}_{on} \; -\overline{\alpha}_{on} \\ & & \overline{\alpha}_{on} \end{array}\right] \tag{3.27}$$

.

$$B = \left[\begin{array}{cc|c} 1 & & \\ -1 & 1 & \\ \ddots & \ddots & \\ \hline & -1 \; 1 & 1 \\ & \ddots \; \ddots & \\ & -1 \; 1 & \\ \hline & & -1 \; 1 \\ & & \ddots \; \ddots \\ & -1 & -1 \; 1 \\ \hline & & \ddots \; \ddots \\ & & -1 \; 1 \\ & & -1 \end{array}\right]. \tag{3.28}$$

3.3.3 Frequency Control Strategy for Aggregated TCLs

In subsection 3.3.2, we present the state space model for aggregation of TCLs after introducing the TCL transport model. The next step is to control aggregated TCLs to regulate frequency f within lower bound (f_{min}) and upper bound (f_{max}). In normal operation, TCLs are controlled by switching between on and off statuses to stay in temperature range $[\theta_i^-,\ \theta_i^+]$; a TCL switches off when its temperature θ_i reaches the lower threshold ($\theta_i \leq \theta_i^-$), and switches on when it reaches the upper threshold ($\theta_i \geq \theta_i^+$). In control of TCLs the lockout effect as stated in (3.10) is also considered to prevent the frequent switching of TCLs. Two issues should be addressed in control of aggregated TCLs. One is how to specify the order that TCLAs should participate in frequency regulation; The other is to determine how the TCLA setting temperature and MG frequency deviation are related to each other. These issues are discussed as follows.

Priority list method: When frequency deviation occurs, the population of TCLs should change their power consumption in a prioritized order [35]. For all aggregators, priority list is determined according to the TCLA setting temperature distance to TCLA setting temperature boundary, i.e., by

$$\pi_k(t) = (\theta_{set,k}(t) - \theta^-_{set,k})/\Delta_{db,k}, \qquad f < f_0 \tag{3.29a}$$

$$\pi_k(t) = (\theta^+_{set,k} - \theta_{set,k}(t)/\Delta_{db,k}, \qquad f > f_0 \tag{3.29b}$$

where $\pi_k(t)$ is the priority list index of k^{th} aggregator at time t, $\theta_{set,k}(t)$ is TCLA setting temperature of k^{th} aggregator at time t, $\theta^-_{set,k}$ and $\theta^+_{set,k}(t)$ are lower and upper bound of TCLA setting temperature of k^{th} aggregator, $\Delta_{db,k}$ is width of the temperature dead-band for k^{th} aggregator, and f_0 is the normal system frequency. The on and off TCLs are ordered according to (3.29a) and (3.29b), respectively. The temperature setting of TCLA with the highest priority will be adjusted first, and then temperature setting of TCLAs with lower priorities will be considered in sequence until the desired regulation is achieved. This priority stack-based control strategy is to increase the comfort level of customers while doing the frequency regulation.

Temperature-frequency control: As the k^{th} TCLA is chosen according to priority list method for frequency regulation, its setting temperature will be adjusted according to temperature-frequency control method [38]. This control method works according to a relation between MG frequency and TCLA setting temperature. The temperature fluctuates around the user-defined setpoint $\theta_{set,k}$, which is equal to the steady state temperature $\hat{\theta}_0$ at normal operation. TCL control is to determine how the TCLA temperature setting $\theta_{set,k}$ should be adjusted as a function of MG frequency f, indirectly controlling the power consumption level. It specifies the existence of a deadband around the nominal system frequency f_0 in which the temperature shall remain unaffected. We denote this deadband by interval $[f_0^-, f_0^+]$, where $f_0^- \leq f_0 \leq f_0^+$. When the system frequency exceeds this deadband, the TCLAs should adjust their setpoints in proportion to the frequency deviation. The limits of the controllable setpoint range ($\theta^-_{set,k}$ and $\theta^+_{set,k}$) should be reached at the statutory limits of the

system frequency range. The relation between frequency and temperature can be represented by [38]

$$\theta_{set,k} = \begin{cases} \theta^{+}_{set,k}, & f \leq f_{min} \\ \hat{\theta}_0 + \dfrac{(\theta^{+}_{set,k} - \hat{\theta}_0)(f_0^- - f)}{f_0^- - f_{min}}, & f_{min} < f < f_0^- \\ \hat{\theta}_0, & f_0^- \leq f \leq f_0^+ \\ \hat{\theta}_0 + \dfrac{(\theta^{-}_{set,k} - \hat{\theta}_0)(f - f_0^+)}{f_{max} - f_0^+}, & f_0^+ < f < f_{max} \\ \theta^{-}_{set,k}, & f \geq f_{max}. \end{cases} \tag{3.30}$$

During normal operation, TCLs in the k^{th} aggregator under the constraint of (3.10) switch off/on at the thresholds θ_k^- and θ_k^+ which are the lower and upper limit of the temperature deadband around the setting temperature $\theta_{set,k}$ given by

$$\theta_k^- = \theta_{set,k} - \Delta_{db,k}, \quad \theta_k^+ = \theta_{set,k} + \Delta_{db,k}. \tag{3.31}$$

A basic frequency response can be implemented by making one or both thresholds dependent on the system frequency. In the following, we focus on compensating for the frequency drop by adjusting TCLA setting temperature. To this end, we keep the upper threshold θ_k^+ constant, and we use a dynamic lower threshold $\theta^{-}_{set,k}$, with $\theta^{-}_{set,k}(f_0) = \theta_k^-$. For simplicity, the steady state distribution of TCLs is considered uniform over the range $[\theta_k^-, \theta_k^+]$. Furthermore, we assume that the full range of temperatures is accessible to the controller, so that $\theta^{+}_{set,k} = \theta_k^+$. As a result, we can make the following approximation for the desired frequency dependence of $\theta^{-}_{set,k}(f)$

(for $f \leq f_0$)

$$\theta^-_{set,k} = \begin{cases} \theta^+_k, & f \leq f_{min} \\ \theta^-_k + \dfrac{(\theta^+_k - \theta^-_k)(f^-_0 - f)}{f^-_0 - f_{min}}, & f_{min} < f < f^-_0 \\ \theta^-_k, & f^-_0 \leq f \leq f_0. \end{cases} \tag{3.32}$$

In case of a loss-of-generation event, $\theta^-_{set,k}(f)$ increases rapidly and any available TCL with a temperature less than $\theta^-_{set,k}(f)$ will be switched off immediately, which results in a rapid and significant response. A similar approach can be used for the loss of load or the generation rise event.

Algorithm 1 presents the procedure of TCL aggregation model to control the frequency of islanded MG. The algorithm collects the system parameters (e.g., number of TCL, number of aggregator, ambient temperature, etc.) from TCLs. Then, it clusters TCLs into aggregators based on parameters presented in Table 3.1. In this algorithm, the algorithm initializes state variable such as $\dot{\theta}_{set,k} = 0$, and calculates power consumption in each aggregator. In the next step, algorithm checks the frequency deviation of islanded MG, and then prioritize TCLAs based on the setting temperature distance to the TCLA setting temperature boundary. Next, setting temperature for the chosen TCLA is updated based on (3.30). For the small sampling periods (τ), we make an approximation to calculate the input of state space model in (3.26). We determine the number of on/off TCL in each bin for the chosen TCLA based on (3.13) with the consideration of lock-out effect in (3.10). The lock-out constraint prevents TCLs from switching on/off frequently which changes the

number of on/off TCLs in each bin. Next, all required matrices for the state space model are updated, and then consumption power of chosen aggregator for the next step is calculated. Next, demand response power is achieved by change in output power of chosen TCLA. We have considered the DZ as a back-up for cases that DR is not able to provide the required frequency regulation service. Hence, the TCL aggregation control process is continued until DR is available and frequency is back to its range. If DR is not available, DZ will provide the additional regulation service to maintain the MG frequency within the desired range.

3.4 Summary

We consider an aggregation model where all TCLs are clustered and controlled by several aggregators. These aggregators have two-way communication with the MGCC. The MGCC coordinates frequency control with TCLAs participation in accordance with generation side, such that load changes and intermittency of the renewable energy resources are addressed. Moreover, the lockout effect of the TCLs should be considered in order to prevent frequent switching of TCLs which leads to their diminishing life-cycle. In this research, the main parameter in controlling the TCLs switching actions is the temperature setting which has a relation with system frequency. TCLs should be prioritized according to their availability and temperature conditions. Temperature setting is controlled such that TCLs with higher priority participate in frequency control first. This control scheme aims to keep the frequency

as close as possible to its desired range.

Algorithm 1 The proposed TCL operation and control

1: **Input:**
2: System parameters: $\theta_a, \tau, f_0, f_0^-, f_0^+, n_k, n_a, C_{i_k}, R_{i_k}, T_{up,i_k}, T_{down,i_k}, P_{r,i_k}, RU, RD, \Delta_{db,k}$, $i_k \in \Psi_k$, $k \in \{1, ..., n_A\}$
3: State variables: $f, \theta_{set,k}$
4: **Process:**
5: Cluster TCLs based on parameters in Table 3.1 into k aggregators, $k \in \{1, ..., n_A\}$
6: Initialize $\dot{\theta}_{set,k} = 0$ and $t = 0$, $k \in \{1, ..., n_A\}$
7: Calculate $P_{TCL,k}(t)$ based on state-space model of (3.26), $k \in \{1, ..., n_A\}$
8: **if** $|\Delta f| > |f - f_0^+|$ **then**
9: **if** $f < f_0^-$ **then**
10: Calculate $P_{DZ}(t+\tau) = \Delta P_{DZ}(t) + RU \cdot \tau$
11: Prioritize TCLAs by $\pi_k(t) = (\theta_{set,k}(t) - \theta_{set,k}^-)/\Delta_{db,k}$
12: **else**
13: Calculate $P_{DZ}(t+\tau) = \Delta P_{DZ}(t) - RD \cdot \tau$
14: Prioritize TCLAs by $\pi_k(t) = (\theta_{set,k}^+ - \theta_{set,k}(t))/\Delta_{db,k}$
15: Assign k_{low} to index of the lowest $\pi_k(t)$ value
16: Calculate $\theta_{set,k}^-(t+\tau), \theta_{set,k}^+(t+\tau)$ based on (3.32), $k = k_{low}$
17: Calculate $\theta_{set,k}(t+\tau)$ based on (3.30), $k = k_{low}$
18: Calculate $\dot{\theta}_{set,k} \approx (\theta_{set,k}(t+\tau) - \theta_{set,k}(t))/\tau$, $k = k_{low}$
19: Determine $X_{on/off}(t, \theta)$ based on (3.13) considering lock-out effect in (3.10)
20: Update matrices A, B, C in state-space model in (3.27 and 3.28)
21: Calculate $P_{TCL,k}(t+\tau)$ based on state-space model of (3.26), $k \in \{1, ..., n_A\}$
22: Determine $\Delta P_{DR} = P_{TCL,k}(t+\tau) - P_{TCL,k}(t)$
23: Calculate f from supply-demand balance equation in (3.5)
24: $t \leftarrow t + \tau$
25: **goto** *step 8.*
26: **else**
27: **Output:** $f^{new}, \theta_{set,k}$ for $k \in \{1, ..., n_A\}$

Chapter 4

Performance Evaluation

In this chapter, we evaluate the performance of the aggregation model and the proposed frequency control strategy for the islanded MG. The proposed scheme deals with the transient response for a desired operation, considering frequency control under coordination of the supply and demand sides. Both under-frequency and over-frequency cases are considered. During these cases of frequency regulation, the coordination of MG generation and DR side need to be verified. We evaluate the efficiency of the presented TCL aggregation model by comparing the results with the basic TCL model. Moreover, the effect of lockout is investigated in more detail. At the final step, the performance of the proposed aggregation control model is studied under intermittent behavior of the renewable energy. Numerical results are presented to assess the effectiveness of the proposed model. We ignore any existing communication delays in our system.

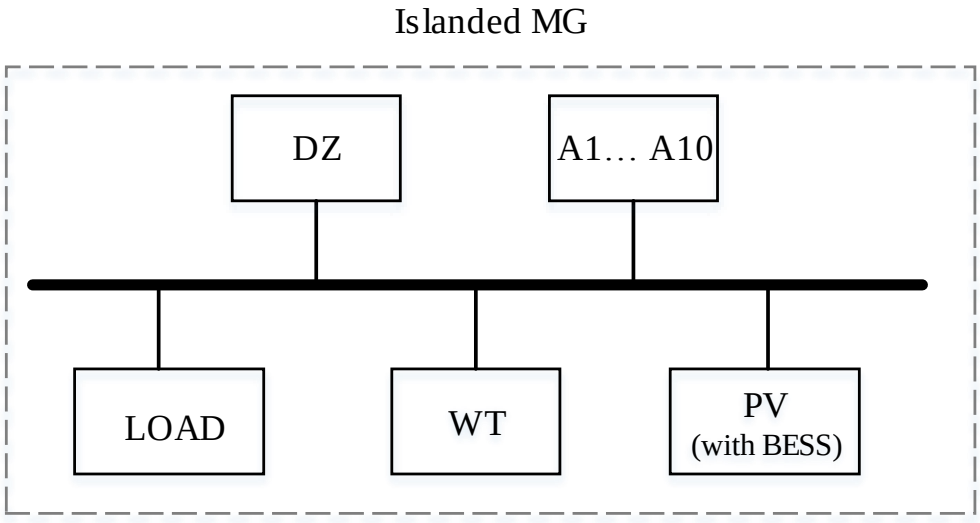

Figure 4.1: Simple islanded MG under consideration.

4.1 Computer simulation model and discussion

An islanded MG including 1) a synchronous DZ, 2) solar generation equipped with battery energy storage system (BESS) and 3) wind generation on the supply side and 4) responsive (i.e., TCLs) and 5) non-responsive loads on the demand side as shown in Figure 4.1 is simulated in the MATLAB/SIMULINK environment to validate the proposed strategy. We assume there exist a large population of TCLs (cooling ACs) in the load section, which are distributed in the MG, and this portion equals to 20% of the total load. Ten TCLAs are assumed to aggregate TCLs in the islanded MG. The parameters regarding the TCLAs are given in Table 4.1. The setting temperatures of the terminal TCLs are provided by MGCC via TCLAs in real time

based on the proposed hierarchical centralized control algorithm. As mentioned in section 3.3.2, the contribution of an individual TCL is not significant, however the aggregated TCLs can have remarkable contribution in frequency regulation. In this regard, a population of 1000 TCLs is aggregated to perform considerable frequency control service. In our simulation, TCLs are rated at 3 kW electrical power. Due to the heterogeneity, thermal resistance R and thermal capacitance C of the TCLs are varied in the range of [1.5,...,2.5] $^{\circ}C/kW$ and [1.5,...,2.5] $kWh/^{\circ}C$. Then, TCLs are grouped into ten clusters using K-means method [39], based on their parameters R and C. The initial setting temperatures $\theta_{set,0}$ for the TCLAs are listed in Table 4.1. Accordingly, the initial temperature $\theta_{i,0}$ for TCLs is chosen randomly within the initial temperature deadband (i.e., $\theta^{-}_{i,0} \leq \theta_{i,0} \leq \theta^{+}_{i,0}$). We assume a total load of 13 MW, out of which 2.6 MW is related to TCLs, and the rest is non-responsive load. Minimum off time and minimum on time for TCLs are set to be $45s$ and $140s$ respectively. A DZ with capacity of 14.11 MW output is the primary source of generation in the system. The installed capacity for PV and WT is set at 1 MW and 1.5 MW respectively. PV panels are equipped with a BESS with capacity of $4000Ah$. Approximately 80% of the TCLs are in ON state, which equal to 1.863 MW. The lower and upper thresholds f_0^{-} and f_0^{+} for frequency regulation, as discussed in Chapter 3 are considered to be $59.8Hz$ and $60.1Hz$, respectively. We define a frequency control index (FCI) for evaluation of the TCL aggregation control strategies. It is computed by the integrating the absolute value of frequency deviation with respect to its desired value f_0 over a time span of the simulation period, given by

$$FCI = \int_0^{t_s} |f - f_0| \, dt \tag{4.1}$$

where $f_0 = 60Hz$ in our study, and t_s is the end of simulation period.

Table 4.1: TCLAs' parameters

Agg.	N_L	$R[°C/kW]$	$C[kWh/°C]$	$P_r[kW]$	$\theta_{set,0}[°C]$	$\Delta_{db}[°C]$
1	87	2.3	1.5	2.736	23.75	0.5
2	118	1.6	1.8	2.394	23.75	0.5
3	146	2.4	2.5	2.223	24.25	0.5
4	75	2.1	2.2	2.565	24.75	0.5
5	99	2.2	1.8	2.736	24.75	0.5
6	129	1.8	2.5	2.907	23.95	0.5
7	47	2.0	1.9	3.078	23.15	0.5
8	79	2.2	2.3	2.565	24.35	0.5
9	96	2.1	2.1	2.394	24.65	0.5
10	124	1.9	1.6	2.736	24.15	0.5

4.2 Numerical results

The performance of the proposed hierarchical centralized frequency control strategy is validated in this section.

A. Performance of the proposed model under load changes: In order to investigate the performance of the proposed model in both under-frequency and over-frequency scenarios, consider that at $t = 5s$ a load of 0.5 MW is added to the system, and at $t = 55s$ a load of 0.4 MW is detached from the system. The load change pattern is shown in Figure 4.2. There is no intermittent behaviour of the generations side, as

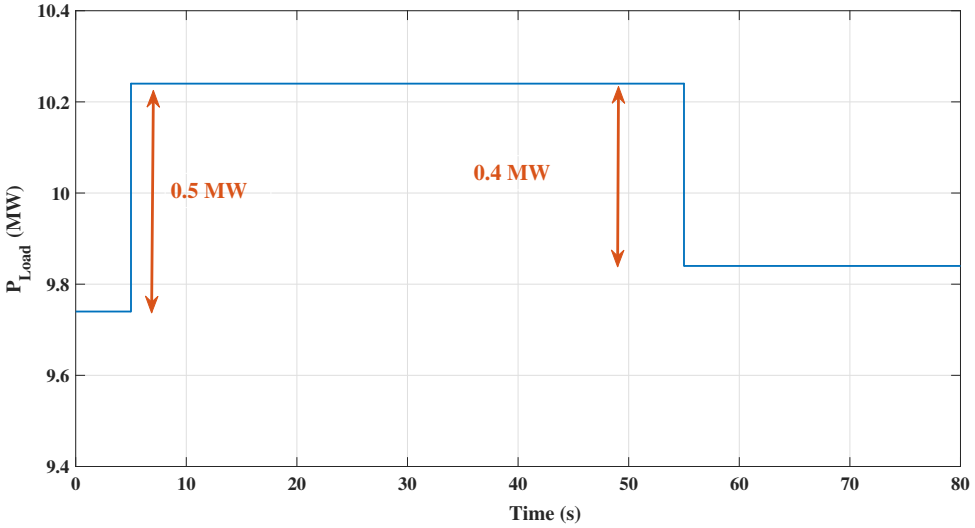

Figure 4.2: Load change pattern.

we study the frequency change and performance of the proposed model for frequency control only due to load changes. In this regard, the PV and WT generation is set to be 0 MW. Figure 4.3 shows as can be seen, using the TCL aggregation control method, frequency is brought back to the normal range in a less time, in comparison with that of basic aggregation control model. The FCI for scenarios of proposed TCL control and basic TCL control is calculated as 4.29 and 6.87, respectively. Obviously, the less the FCI, the better the frequency control performance. Consequently, the results confirm the positive impact of the proposed TCL control method. This is because aggregated TCLs have faster response than sending signals to 1000 TCLs individually. Next, we analyze the results associated with proposed model in more detail. Figure 4.4 shows the TCL power consumption obtained from the proposed model. A portion of on TCLs with aggregated power of 0.5 MW are turned off right

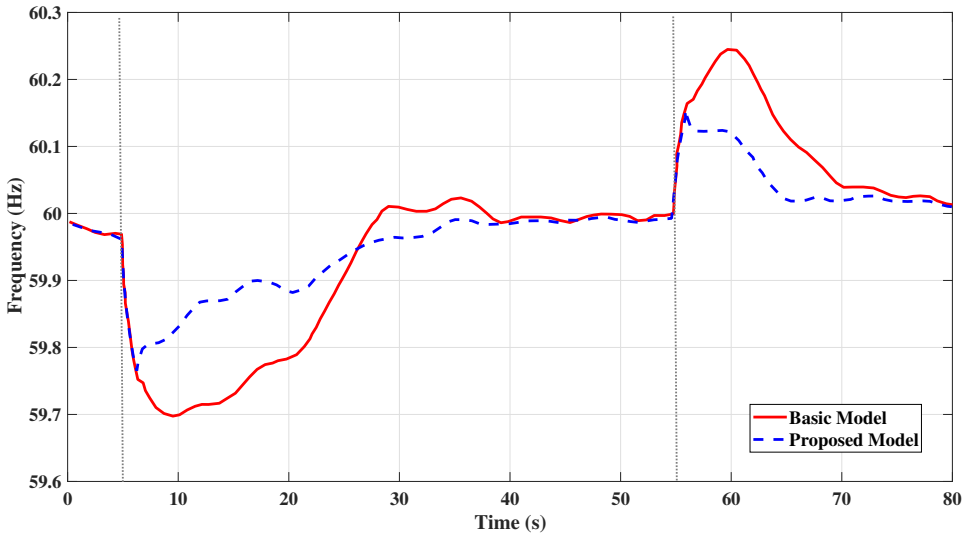

Figure 4.3: Comparison of system frequency response of proposed TCLA control model and basic aggregation model.

after $t = 5s$ to quickly stop the frequency drop. The temperature of those TCLs that are turned off start to increase after they are turned off, and once it is reached to their upper bounds they start to turn on which results in an increasing P_{TCL} level. Moreover, DZ starts to compensate for TCLs power consumption, which causes the diesel power to increase as shown in Figure 4.5.

B. Effect of minimum off time/on time of TCLs on model performance: In this part, we aim to investigate the lockout of TCLs on performance of the proposed model. We perform the simulation in a longer term period $t = [0s, 140s]$ to carefully observe the lockout effect of TCLs. An increase of $0.5MW$ of load occurs at $t = 5s$, which results in a frequency drop as discussed in part A. This causes prioritized TCLs to turn off shortly, and start turning on later if they reach their upper temperature bounds. At $t = 55s$ a loss of load occurs, which causes a frequency increase. This

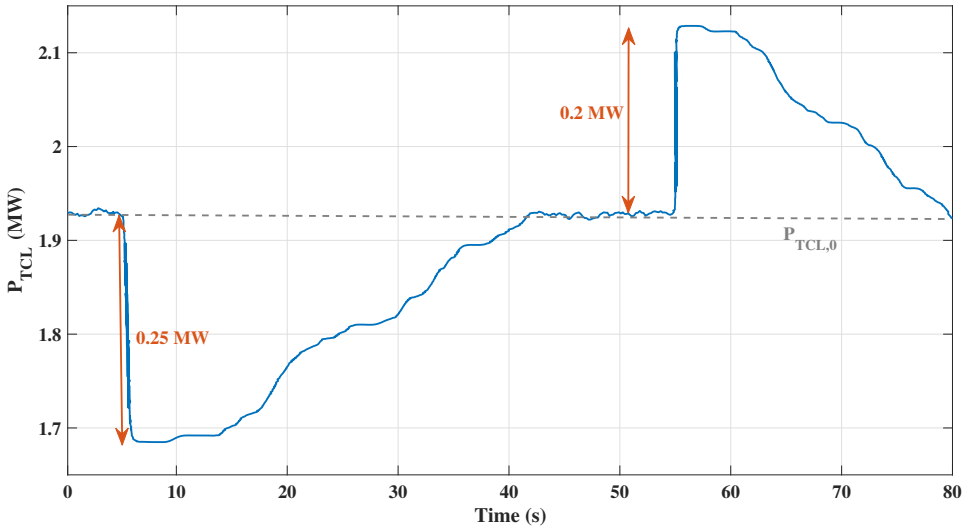

Figure 4.4: active power consumption P_{TCL} of TCLs .

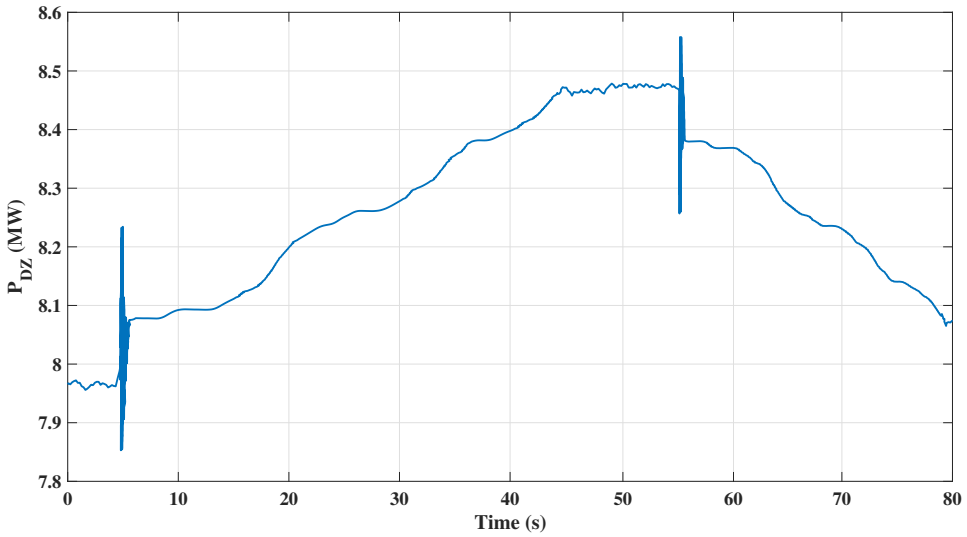

Figure 4.5: DZ active power.

results in OFF TCLs to turn on to compensate for the loss of load. As TCLs are turned on, their temperature moves towards the lower bound, and when reaching the lower bound, they start to turn off. The procedure is similar to what we discuss in part A. Here, in order to evaluate the lockout effect of TCLs more specifically, we add a load increase of 0.4 MW at $t = 90s$. As can be seen in Figure 4.3, the frequency is dropped right after $t = 90s$, which causes some prioritized TCLs to turn off to compensate for the load change. The number of TCLs at $t = 90s$ is considerably less than that at $t = 5s$. This is because those TCLs (which were turned on at $t = 55s$) should keep their status due to lockout and cannot turn off at $t = 90s$. As a result, the frequency drops slightly more than that at $t = 5s$. Figures 4.7 and 4.8 show the power of TCLs and DZ, respectively. The average temperature of TCLs within each aggregator is shown in Figure 4.9. The setting temperature of aggregators A1 and A7 is changed to turn TCLs off at $t = 5s$ to compensate for the load increase, and bring the frequency up to its normal range. At $t = 55s$, aggregator A5 changes its setting temperature to increase P_{TCL}. Later, at $t = 90s$, temperature setting of A4 is changed to reduce P_{TCL}.

C. Performance of the model under intermittent behaviors of renewable energy: Consider a scenario where the intermittent wind power is added to the system. Note that the solar energy is assumed to remain constant in a small portion of time, and we consider a fixed power of 0.25 MW for solar generation. Figure 4.10 shows the wind power with local average over $4s$ periods, which is used in our simulation. The load has a pattern as given in Figure 4.2. Figure 4.11 shows the system frequency response. TCLAs and DZ can bring the frequency close to its desired range, however

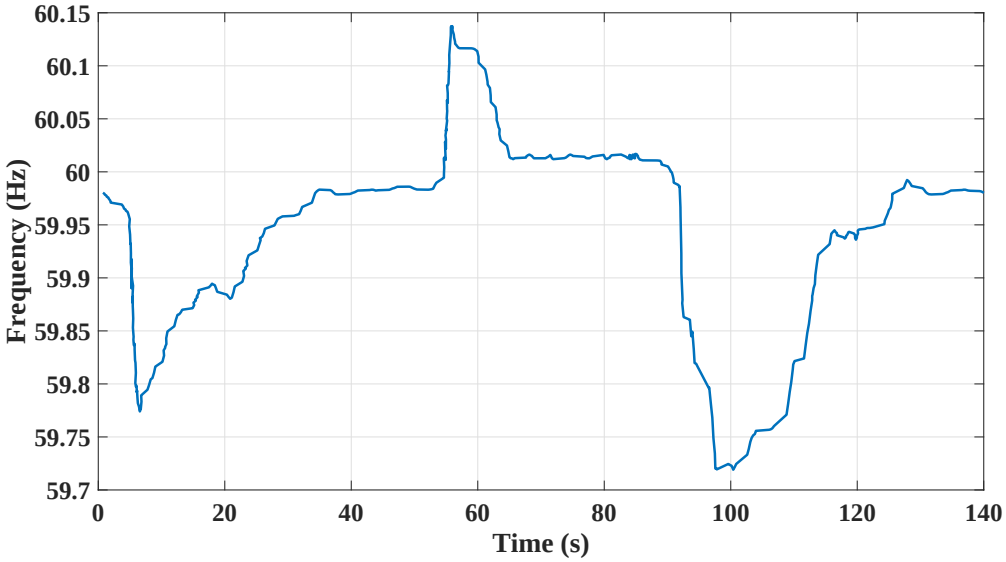

Figure 4.6: Effect of TCL lockout on MG frequency.

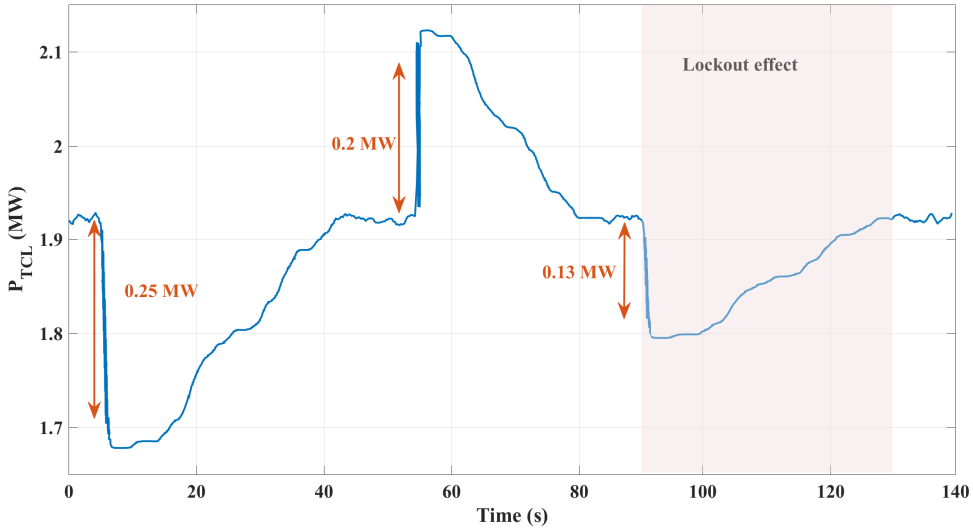

Figure 4.7: Effect of TCL lockout on P_{TCL}.

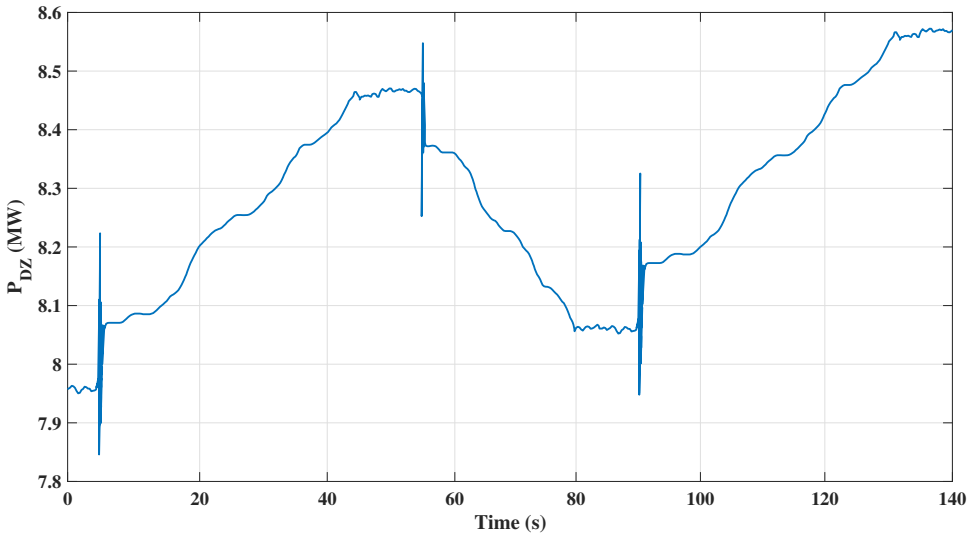

Figure 4.8: Effect of TCL lockout on P_{DZ}.

it comes with distortions that are considerable in system performance. Although TCLAs can act very quickly, it is not desired to turn TCLs on and off frequently, in order to keep the user comfort level and TCL life time in consideration. As a result, we can take advantage of the BESS to resude the frequency deviations. Figure 4.11 shows that the MG frequency when using the BESS has less deviations from the desired value. The frequency comes back to its desired range using power from TCLs, DZ and the BESS. Figures 4.12 and 4.13 show power provided by TCLs and DZ, respectively. As the wind power increases significantly and a loss of load occurs at $t = 55s$, power of TCLs increases and DZ power starts to decrease to provide regulation for the imbalanced power.

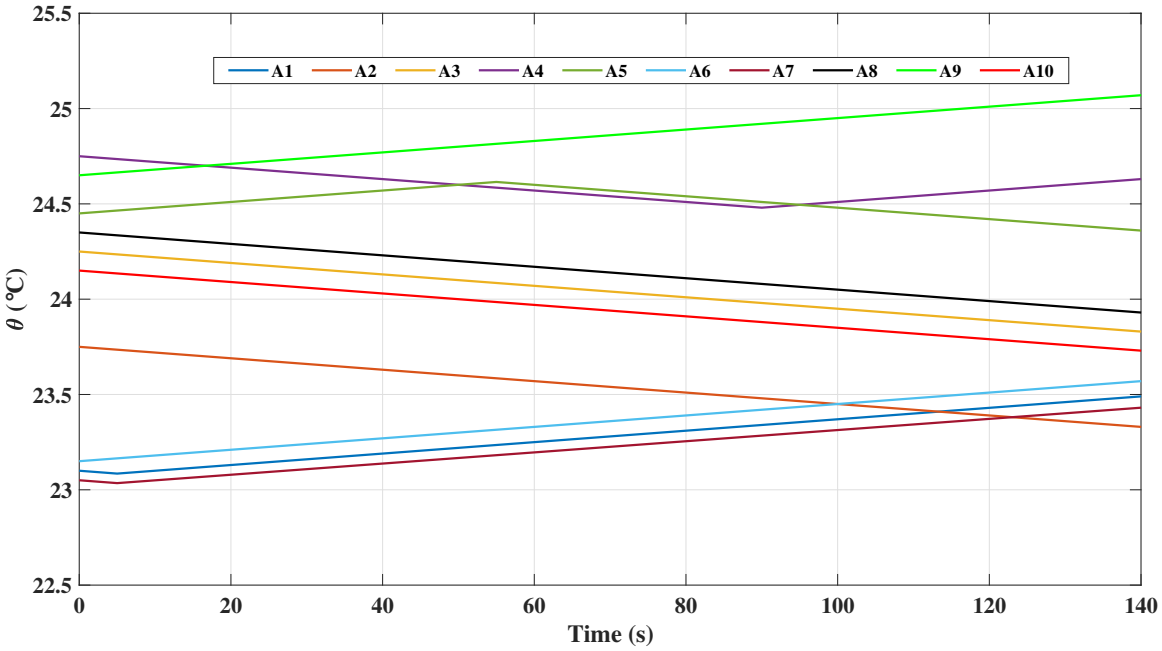

Figure 4.9: Average temperature of TCLAs.

4.3 Summary

In this chapter, we evaluate the performance of the proposed aggregation and control strategy in several scenarios. We first compare the performance of the proposed aggregation model and basic aggregation model. The results show that the evaluation index of FCI is less when using the proposed model. Then, we increase the simulation time to study the effect of minimum off/on time of TCLs on system operation. Results show that, with TCLs particpation in frequency control in a load change event, their availability to compensate for later load-supply imbalances is reduced and DZ has more participation in frequency control, which is necessary to maintain the comfort level of customers as well as lifetime of TCLs. Finally, the performance

of the proposed model is investigated under intermittent behavior of RES. It is concluded that DZ and TCLs cannot compensate for minor changes in load-supply imbalance, and BESS should provide the small regulation needs in such cases.

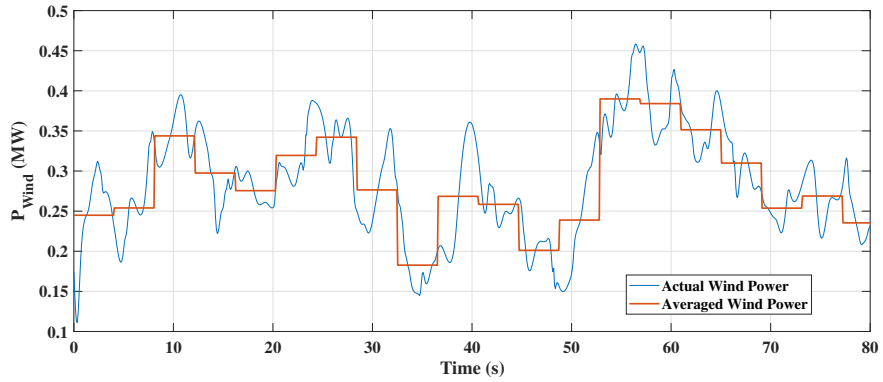

Figure 4.10: Total wind power generation.

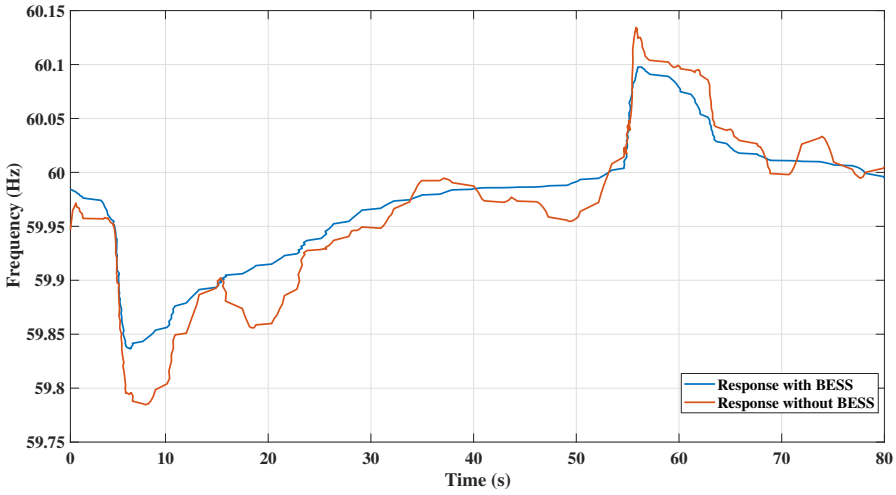

Figure 4.11: MG system frequency under intermittent behavior of RES.

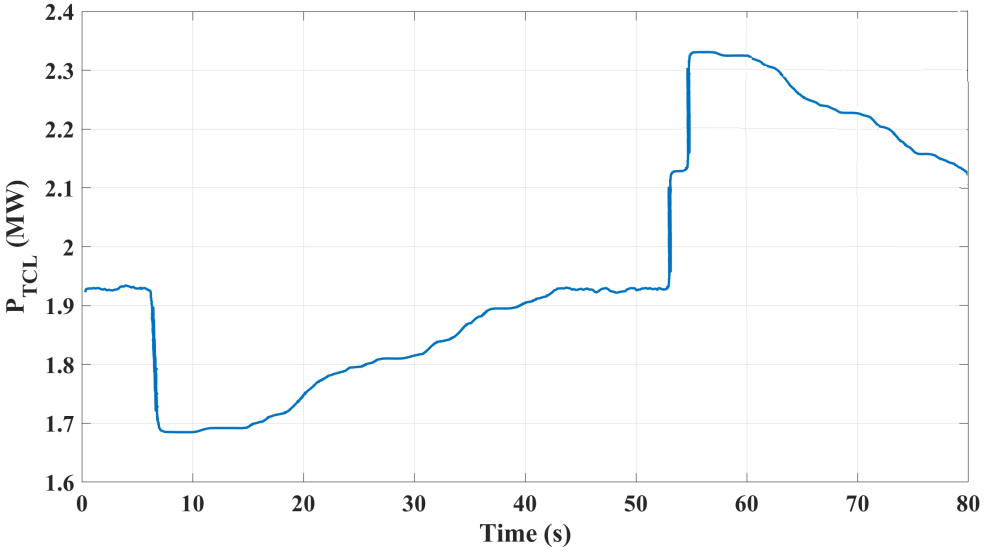

Figure 4.12: TCL power generation under intermittent behavior of RES.

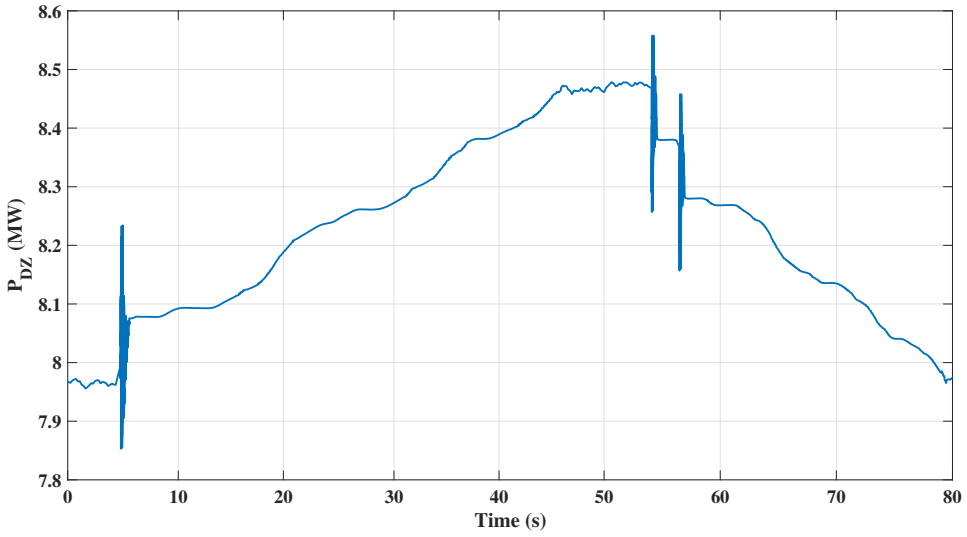

Figure 4.13: DZ power generation under intermittent behavior of RES.

Chapter 5

Conclusion and future work

5.1 Conclusion

DR programs are cost efficient alternative for generation side regulation service providers in MGs. Among all potential responsive devices, TCLs can be considered as a promising choice due to their capability in providing acceptable comfort level to the consumers while under energy consumption control, and their fast acting properties. These devices can be controlled either by directly switching on/off or indirectly by changing their temperature settings. However, while controlling these devices in MGs, several challenges should be addressed. First, an individual TCL is not able to provide a considerable impact on system frequency. Hence, it is imperative to aggregate a large number of TCLs to provide a significant regulation service to the system. This requires to develop an aggregation model which is comprehensive to let a large number of TCLs participate in regulation services. In order to have effective

control over all devices, they can be grouped into several clusters, each handled by a TCLA. The MGCC is in charge of keeping the supply demand balance via TCLAs to provide power for regulation services, whenever needed. It is also important to keep the comfort level of customers as high as possible. Hence, we can prioritize TCLAs' participation, letting those with highest control priority provide the regulation service first. Moreover, in order to prevent frequent switching of TCLs, it is required to consider minimum off/on time of these devices. This causes TCLs to remain in their status (i.e., on or off) for at least a certain duration, after their temperature setting is changed. Providing the prioritized aggregated TCLAs considering the minimum off/on time requires an effective control strategy to act fast in a low inertia islanded MG. A frequency control strategy based on a relation between frequency deviation and temperature setting of TCLAs can be determined to provide required power to keep supply-demand balance. In this thesis, we have considered all the aforementioned concerns, and provided a comprehensive TCL aggregation model and control. This model can act fast taking into account the comfort level of the customers and lifetime of the devices. Our model demonstrates that; 1) because of the lockout effect of TCLs, in presence of chaotic wind power generation, it is essential to take advantage of the BESS to reduce minor frequency deviations in the system; 2) under both under and over frequency scenarios, the proposed frequency control algorithm can act efficiently; and 3) coordination of TCLAs and generation components of the system can provide the frequency regulation service properly. Overall, we can summarize our research contributions as follows:

- We implement clustering TCLs into several groups and handling each with a

TCLA to create a foundation for hierarchical central control strategy, taking into account the thermal dependability of TCLs.

- Aggregation models such as the one in [12] have been mainly used for load following purposes and the relative case studies are in a time scale of minutes to several hours. To the best of the our knowledge, this study is one of a few studies which deal with fast regulation performed by aggregated TCLs in islanded MGs in order of seconds.

- We consider the coordination of generation (renewable-non-renewable) and DR in an islanded MG, instead of simply using the load-supply balancing signal from the power system operator. We also study the lockout effect of individual TCLs to make the model more cost efficient and executable.

5.2 Future work

In this thesis, although we consider a few number of challenges regarding frequency control via aggregated TCLs in an MG, some other research issues remain open for future work. The communication delay in MG frequency control can have a significant impact on behavior of the regulation providers. This can be an important future research problem especially in providing regulation service using several TCLAs in our system. Moreover, in our model, we use first order modeling of TCLs. The second order TCL model includes building mass temperature and can be evaluated for more detailed TCL aggregation models. Finally, similar to a TCL, an EV is

the other potential candidate in MGs to provide regulation service. How to aggregate and control electric vehicle (EV)s to take advantage of their power energy in regulation services requires further studies.

References

[1] W. Su and J. Wang. Energy management systems in microgrid operations. *The Electricity Journal*, 25(8):45–60, 2012.

[2] N. Hatziargyriou, H. Asano, R. Iravani, and C. Marnay. Microgrids. *IEEE Power and Energy Magazine*, 5(4):78–94, 2007.

[3] R. H. Lasseter, C. M. A. Akhil, J. D. J. Stephens, R. Guttromson, A. Meliopoulous, and R. J. Yinger. The certs microgrid concept. Technical report, Transmission Reliability Program, Office of Power Technologies, US Department of Energy, 2002.

[4] A. Molina-Garcia, F. Bouffard, and D. S. Kirschen. Decentralized demand-side contribution to primary frequency control. *IEEE Transactions on Power Systems*, 26(1):411–419, 2011.

[5] Y. G. Rebours, D. S. Kirschen, M. Trotignon, and S. Rossignol. A survey of frequency and voltage control ancillary services—part i: Technical features. *IEEE Transactions on power systems*, 22(1):350–357, 2007.

[6] Y. G. Rebours. Some salient features of the management of frequency and voltage control ancillary services. In *Power Engineering Society General Meeting*, pages 1–6. IEEE, 2007.

[7] M. Amini and M. Almassalkhi. Investigating delays in frequency-dependent load control. In *Innovative Smart Grid Technologies-Asia (ISGT-Asia)*, pages 448–453. IEEE, 2016.

[8] M. Amini and M. Almassalkhi. Trading off robustness and performance in receding horizon control with uncertain energy resources. In *Power Systems Computation Conference (PSCC)*, 2018.

[9] Y. Guo, L. Zhang, J. Zhao, F. Wen, A. Salam, J. Mao, and L. Li. Networked control of electric vehicles for power system frequency regulation with random communication time delay. *Energies*, 10(5), 2017.

[10] W. Yao, J. Zhao, F. Wen, Y. Xue, and G. Ledwich. A hierarchical decomposition approach for coordinated dispatch of plug-in electric vehicles. *IEEE Transactions on Power Systems*, 28(3):2768–2778, 2013.

[11] J. Hu, J. Cao, M. Z. Q. Chen, J. Yu, J. Yao, S. Yang, and T. Yong. Load following of multiple heterogeneous tcl aggregators by centralized control. *IEEE Transactions on Power Systems*, 32(4):3157–3167, 2017.

[12] S. Bashash and H. K. Fathy. Modeling and control of aggregate air conditioning loads for robust renewable power management. *IEEE Transactions on Control Systems Technology*, 21(4):1318–1327, 2013.

[13] N. Lu. An evaluation of the hvac load potential for providing load balancing service. *IEEE Transactions on Smart Grid*, 3(3):1263–1270, 2012.

[14] D. S. Callaway and I. A. Hiskens. Achieving controllability of electric loads. *Proceedings of the IEEE*, 99(1):184–199, 2011.

[15] M. R. V. Moghadam, R. T. Ma, and R. Zhang. Distributed frequency control in smart grids via randomized demand response. *IEEE Transactions on Smart Grid*, 5(6):2798–2809, 2014.

[16] J. Wang, H. Zhang, and Y. Zhou. Intelligent under frequency and under voltage load shedding method based on the active participation of smart appliances. *IEEE Transactions on Smart Grid*, 8(1):353–361, 2017.

[17] N. Lu and D. P. Chassin. A state-queueing model of thermostatically controlled appliances. *IEEE Transactions on Power Systems*, 19(3):1666–1673, 2004.

[18] J. M. Guerrero, M. Chandorkar, T. L. Lee, and P. C. Loh. Advanced control architectures for intelligent microgrids—part i: Decentralized and hierarchical control. *IEEE Transactions on Industrial Electronics*, 60(4):1254–1262, 2013.

[19] C. H. Lo and N. Ansari. Decentralized controls and communications for autonomous distribution networks in smart grid. *IEEE Transactions on Smart Grid*, 4(1):66–77, 2013.

[20] E. Planas, A. Gil de Muro, J. Andreu, I. Kortabarria, and I. M. de Alegria. General aspects, hierarchical controls and droop methods in microgrids: A review. *Renewable and Sustainable Energy Reviews*, 17:147–159, 2013.

[21] K. Dehghanpour and S. Afsharnia. Electrical demand side contribution to frequency control in power systems: a review on technical aspects. *Renewable and Sustainable Energy Reviews*, 41:1267 – 1276, 2015.

[22] S. A. Pourmousavi and M. H. Nehrir. Real-time central demand response for primary frequency regulation in microgrids. *IEEE Transactions on Smart Grid*, 3(4):1988–1996, 2012.

[23] L. R. Chang-Chien, L. N. An, T. W. Lin, and W. J. Lee. Incorporating demand response with spinning reserve to realize an adaptive frequency restoration plan for system contingencies. *IEEE Transactions on Smart Grid*, 3(3):1145–1153, 2012.

[24] V. Trovato, I. M. Sanz, B. Chaudhuri, and G. Strbac. Advanced control of thermostatic loads for rapid frequency response in great britain. *IEEE Transactions on Power Systems*, 32(3):2106–2117, 2017.

[25] S. Weckx, R. D'hulst, and J. Driesen. Primary and secondary frequency support by a multi-agent demand control system. *IEEE Transactions on Power Systems*, 30(3):1394–1404, 2015.

[26] M. R. V. Moghadam, R. Zhang, and R. T. Ma. Distributed frequency control via randomized response of electric vehicles in power grid. *IEEE Transactions on Sustainable Energy*, 7(1):312–324, 2016.

[27] M. Aunedi, P. A. Kountouriotis, J. E. O. Calderon, D. Angeli, and G. Strbac. Economic and environmental benefits of dynamic demand in providing frequency regulation. *IEEE Transactions on Smart Grid*, 4(4):2036–2048, 2013.

[28] K. Christakou, D. C. Tomozei, J. Y. Le Boudec, and M. Paolone. Gecn: Primary voltage control for active distribution networks via real-time demand-response. *IEEE Transactions on Smart Grid*, 5(2):622–631, 2014.

[29] Y. Mu, J. Wu, J. Ekanayake, N. Jenkins, and H. Jia. Primary frequency response from electric vehicles in the great britain power system. *IEEE Transactions on Smart Grid*, 4(2):1142–1150, 2013.

[30] G. Benysek, J. Bojarski, R. Smolenski, M. Jarnut, and S. Werminski. Application of stochastic decentralized active demand response (dadr) system for load frequency control. *IEEE Transactions on Smart Grid*, 2017.

[31] Y. Q. Bao, Y. Li, Y. Y. Hong, and B. Wang. Design of a hybrid hierarchical demand response control scheme for the frequency control. *IET Generation, Transmission & Distribution*, 9(15):2303–2310, 2015.

[32] H. Saadat. *Power System Analysis*. McGraw-Hill, 1999.

[33] S. Ihara and F. C. Schweppe. Physically based modeling of cold load pickup. *IEEE Power Engineering Review*, PER-1(9):27–28, 1981.

[34] S. A. Pourmousavi and M. H. Nehrir. Introducing dynamic demand response in the lfc model. *IEEE Transactions on Power Systems*, 29(4):1562–1572, 2014.

[35] H. Hao, B. M. Sanandaji, K. Poolla, and T. L. Vincent. Aggregate flexibility of thermostatically controlled loads. *IEEE Transactions on Power Systems*, 30(1):189–198, 2015.

[36] R. E. Mortensen and K. P. Haggerty. A stochastic computer model for heating and cooling loads. *IEEE Transactions on Power Systems*, 3(3):1213–1219, 1988.

[37] S. Kundu, N. Sinitsyn, S. Backhaus, and I. A. Hiskens. Modeling and control of thermostatically controlled loads. *arXiv preprint arXiv:1101.2157*, 2011.

[38] S. H. Tindemans, V. Trovato, and G. Strbac. Frequency control using thermal loads under the proposed entso-e demand connection code. In *Proceedings of IEEE Eindhoven PowerTech*, pages 1–6, 2015.

[39] J. A. Hartigan and M. A. Wong. Algorithm as 136: A k-means clustering algorithm. *Applied Statistics*, pages 100–108, 1979.